



**The Abdus Salam
International Centre for Theoretical Physics**



2137-6

**Joint ICTP-IAEA Advanced Workshop on Multi-Scale Modelling for
Characterization and Basic Understanding of Radiation Damage
Mechanisms in Materials**

12 - 23 April 2010

Principles of multi-scale modeling

J.M. Perlado
*Universidad Politecnica de Madrid
Spain*

Multiscale Modeling of Irradiated Materials

J. Manuel Perlado
Instituto Fusión Nuclear
Universidad Politécnica Madrid

The two large problems with materials in irradiation environments

- **Activation**

consequence = Radioactivity, with effects in Safety and Environment

- **Damage**

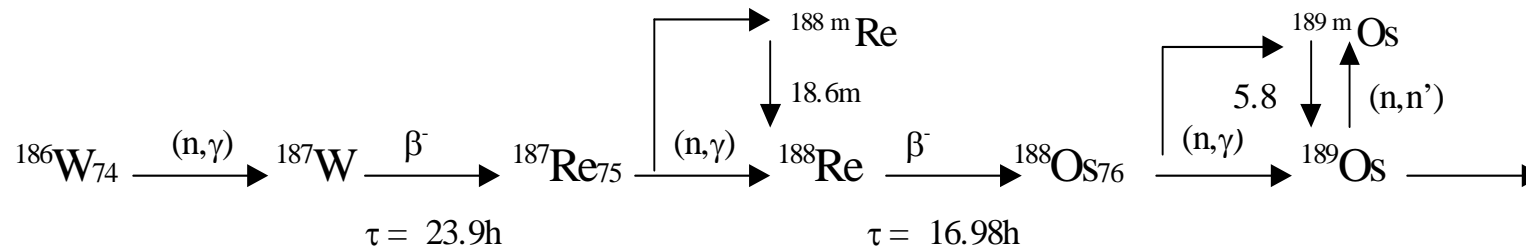
consequence = changes in expected design properties of the materials

- Affecting **Fission, Fusion, Transmutation** systems

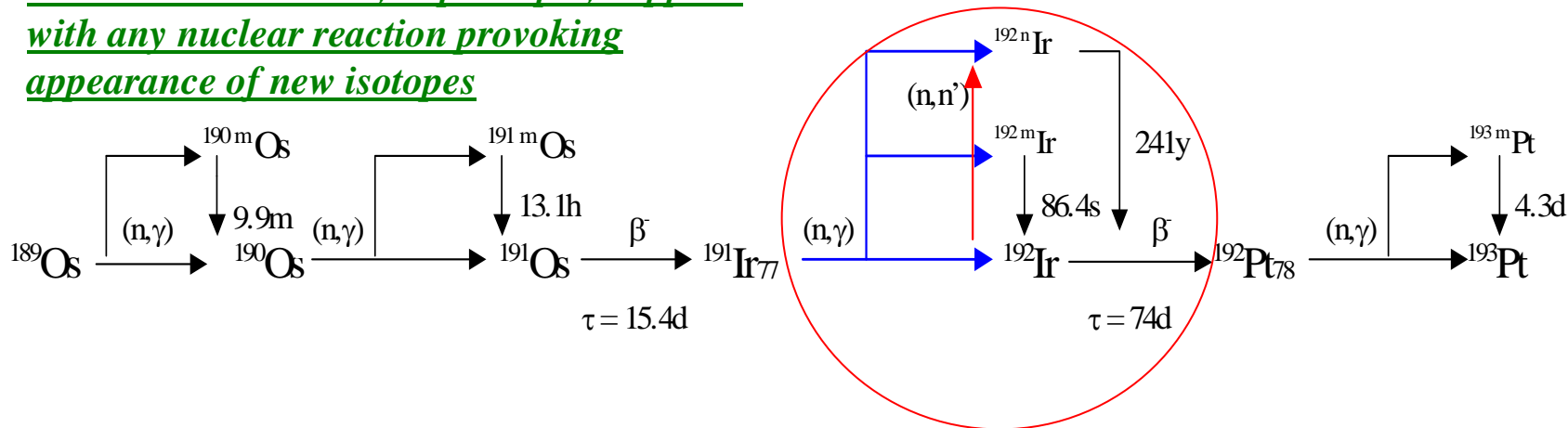
Mechanisms of **Neutron/Gamma / Activation**: Effective chains

Consequences = some of those **generated isotopes** are **Radioactive** with more or less long lifetimes (!!!!!!!!!!!!!!!)

Production of ^{192m}Ir from ^{186}W : Major transmutation/decay chain



“ACTIVATION” can, in principle, happens with any nuclear reaction provoking appearance of new isotopes



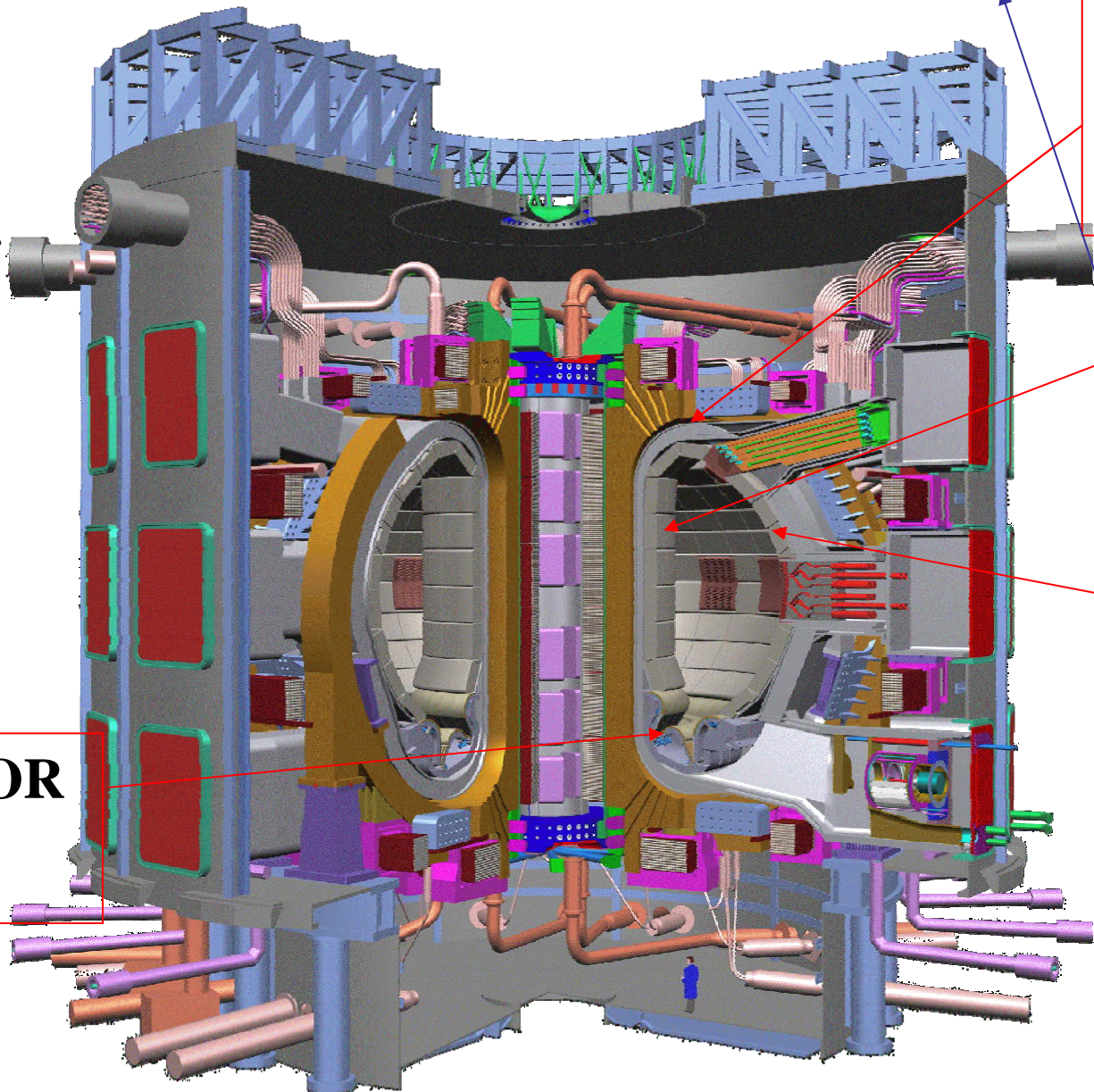
The PROBLEM of the Material in Irradiated Systems depends on:

- **WHERE (?) is the material (type and total fluence received of radiation)**

- **WHICH (?) is the function of the Material**

Hopefully in First Wall NO EFFECT of CP

It is not the same WHO generate a *problem* (activation or damage) in each of the components of the facility here represented



Vacuum Vessel
(NG)

First Wall
(XR+CP)

Blanket
(NG)

DIVERTOR
(CP)

Charged Particles = CP
Neutrons + Gammas = NG
X-Rays radiation = XR

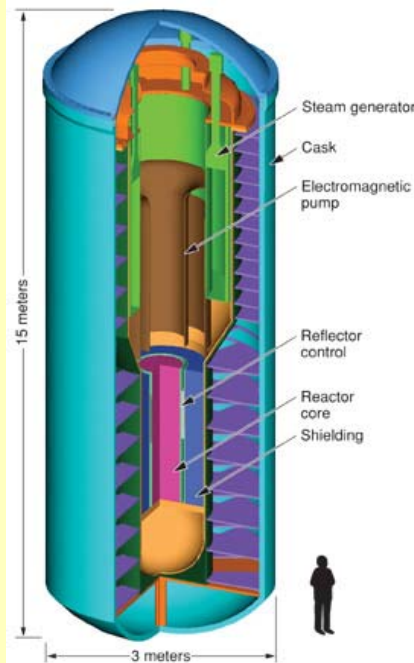
Computational tools for alloys to understand materials under extreme conditions: FISSION

Motivation

Radiation Damage

- Mechanical properties F/M steels

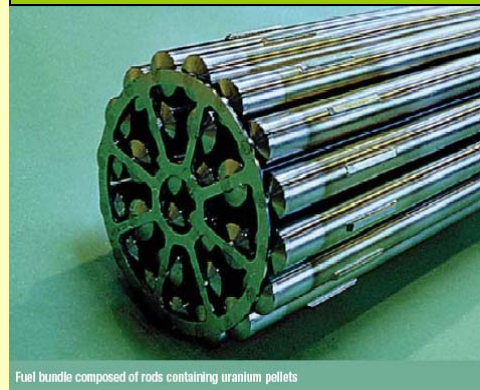
Advanced Burner Reactor



Nuclear materials

- Structural steels (Fe-Cr) / nuclear fuels
- Microstructural evolution under irradiation

Nuclear fuel bundle

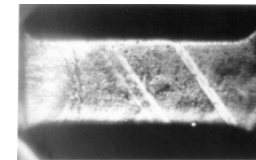


Fuel bundle composed of rods containing uranium pellets

Extreme conditions

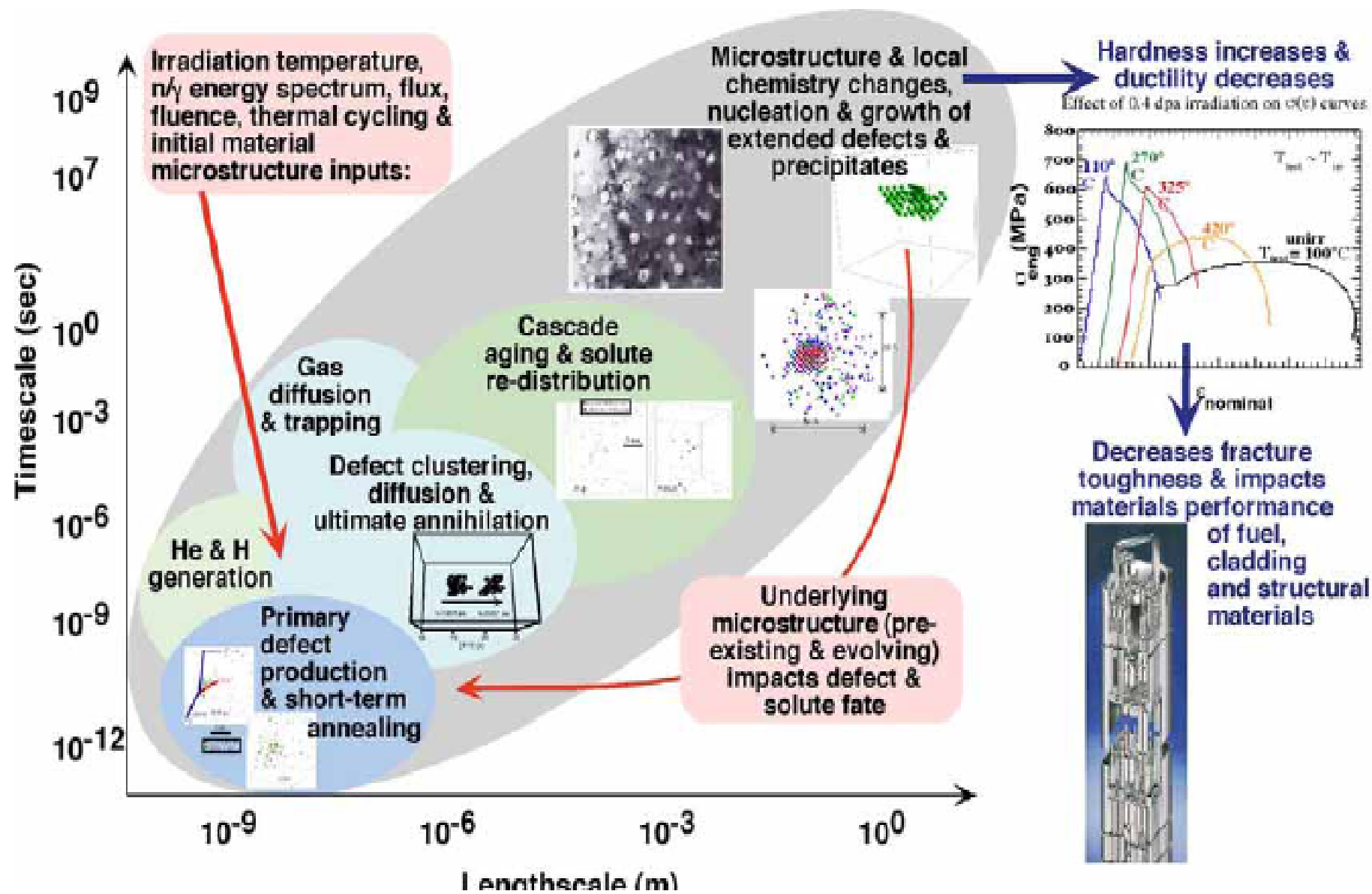
- Dislocation dynamics in alloys
- Predict strain localization and embrittlement in irradiated samples

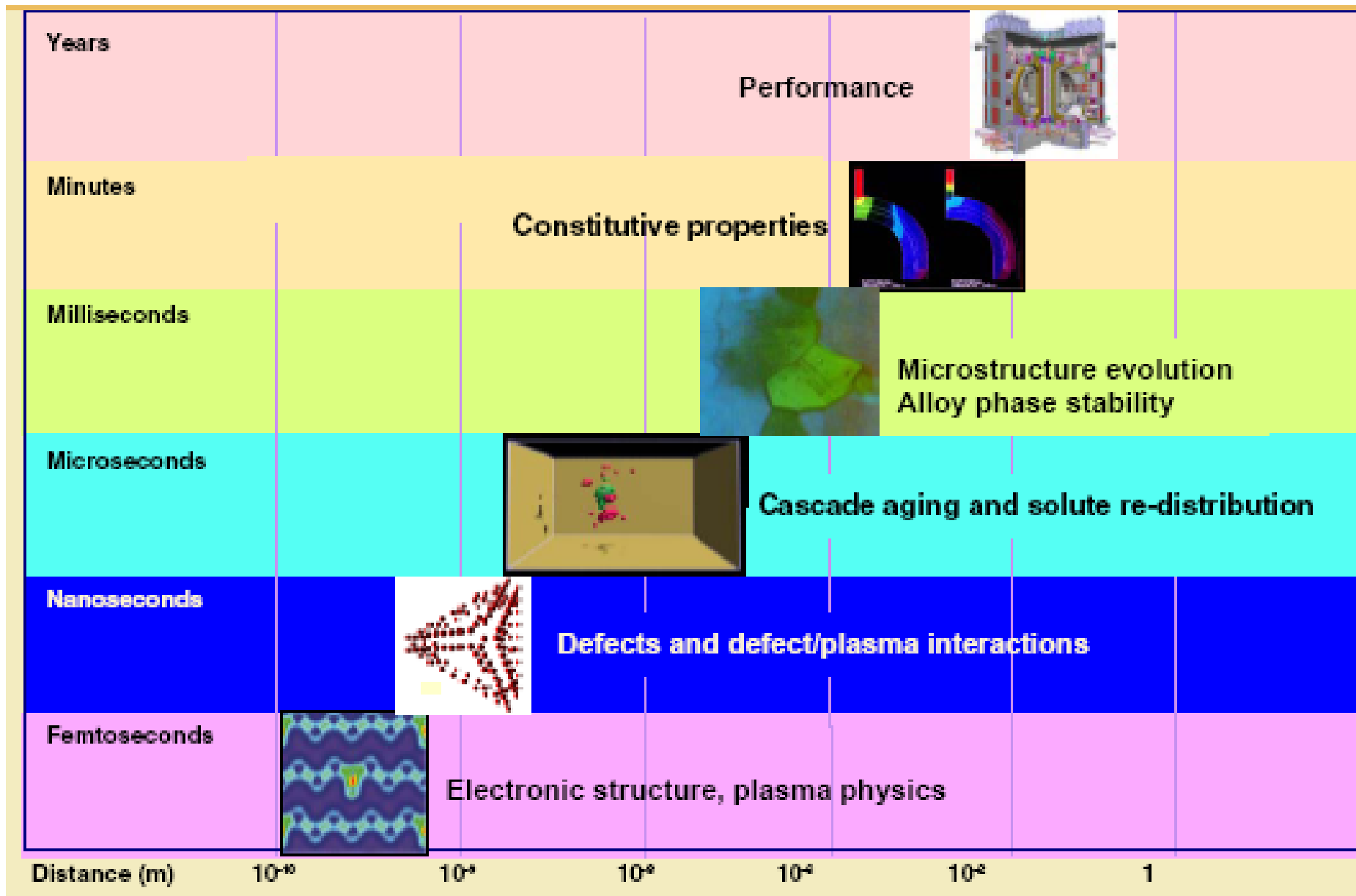
Experiment



Tensile Test Simulation





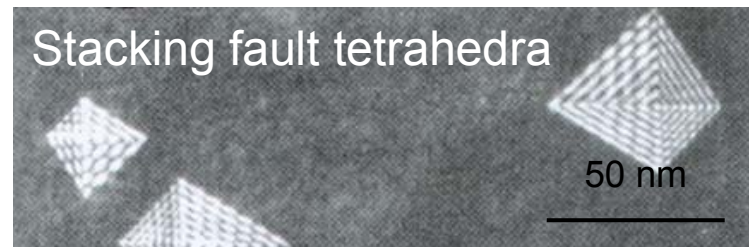


Evolution of the Microstructure

After the generation of defects, those follow annealing /thermal, recombination; diffuse, agglomerate among them, dissociate.....and finally

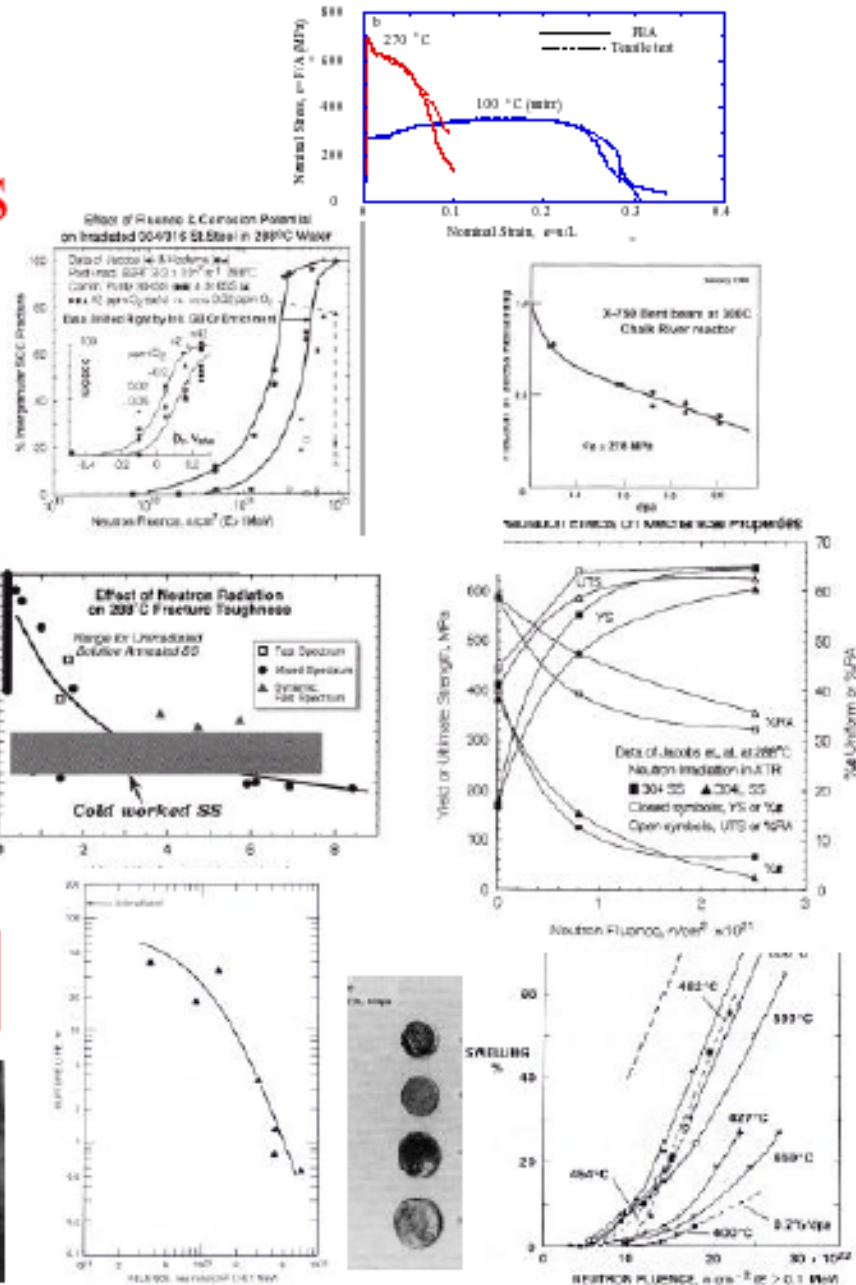
Complex secondary defects:

- Small defect clusters
- Interstitial dislocation loops
- Vacancy dislocation loops
- Stacking fault tetrahedra
- Precipitates
- Voids
- He bubbles



Radiation Effects - Causes & Consequences

- Cause - displacement (dpa) and transmutation damage (specially He and H) coupling with with thermal, stress and chemically driven processes that occur without irradiation
- Dimensional instability creep (stress), swelling & growth
- Lower ductility & creep failure time
- Lower fracture resistance in the presence of cracks
- Enhanced environmentally assisted cracking



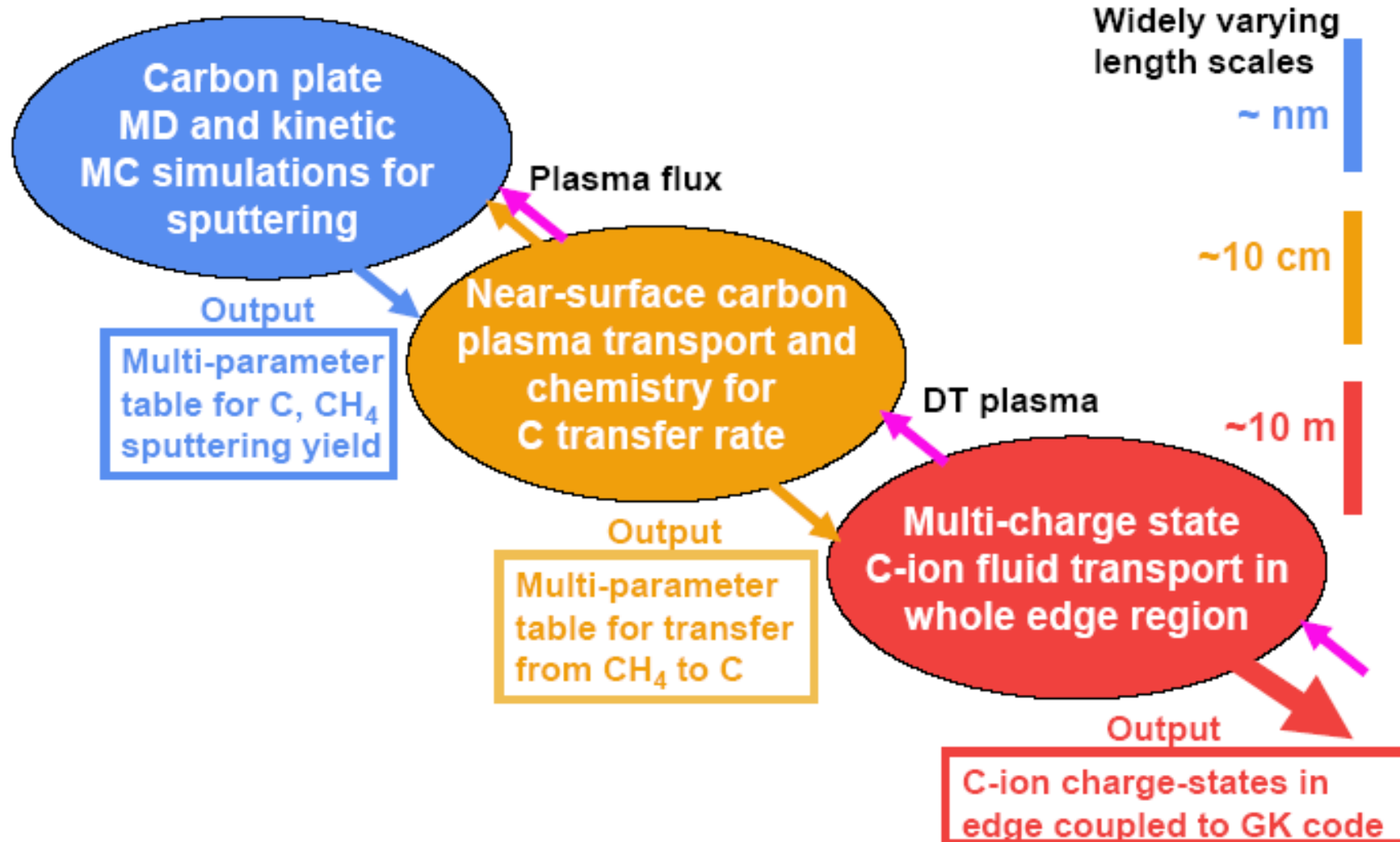
Sequence of Magnitudes to be known in Materials Damage under

NEUTRON or GAMMA Irradiation

- Determination of Neutron/Gamma Source
- Determination of Primary Knock-on Atoms in the material from NUCLEAR reactions
- Basic parameters of damage: dpa and gaseous production
- Atomistic Mechanisms
- Microscopic up to lifetime
- Macroscopic responses under irradiation

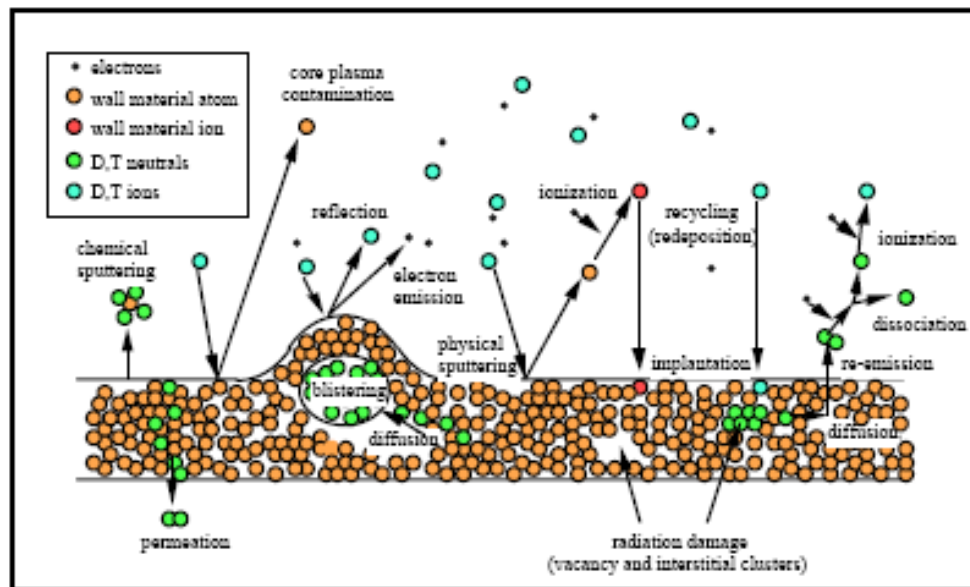
CHARGED PARTICLES IRRADIATION

Impurities in the edge plasma are important for power balance

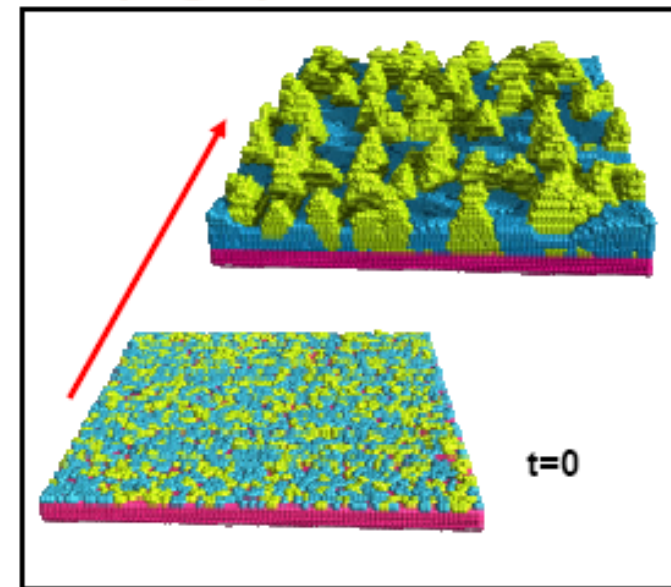


Carbon contamination of the plasma results from erosion of the surface by chemical and physical sputtering.

Divertor surface processes



Topographical evolution



Molecular Dynamics and surface Monte Carlo simulations enable fundamental understanding and determine required sputtering-yield data

The European Programme: **FUSION**

The EU technology programme budget (150 M€/year) is dedicated to:

- ITER design and R&D (70%)
- Long-term activities (30%)
- Areas included in the **Long Term Programme:**

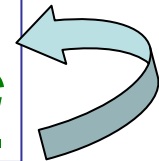
- Breeding Blanket

- **IFMIF**

BROADER APPROACH

- **Materials Development (~ 8 M€/year for R&D) MULTISCALE MODELING**

you see...



- System Studies

- Power Plant Conceptual Study
- Socio-Economic Studies
- Safety and Environment

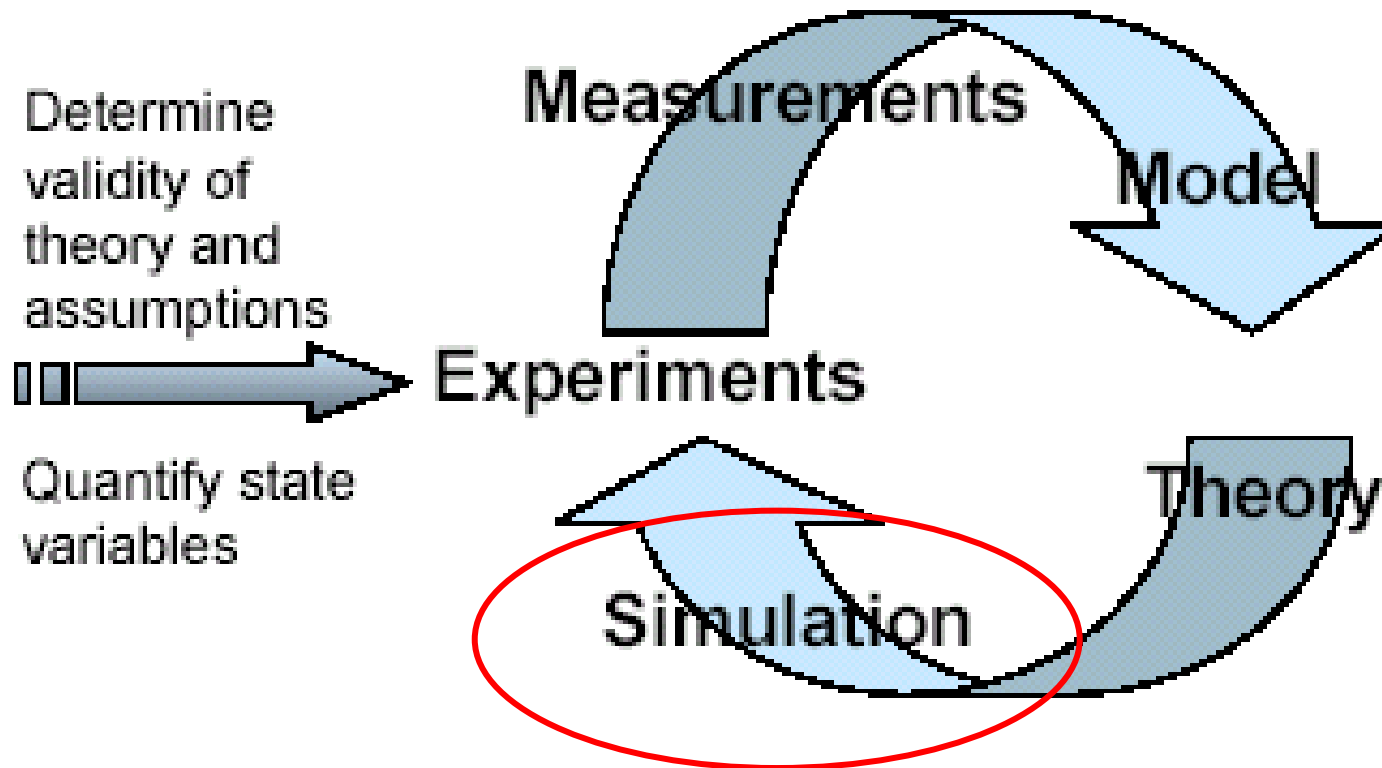
MATERIALS are **KEY** in consideration of medium/long term to **DEMO PP**

EU Materials Development” Programme



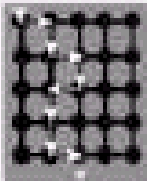






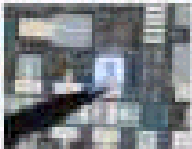




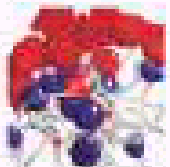

*Other materials to be developed solving **temperature increase and activation** are:*

- (a) **ODS (Oxide Dispersion Strengthened) steels** to improve the performance through an **increased operational temperature window**.*
- (b) **SiC/SiC ceramic composites** as structural material for advanced blanket in the **very long term**.*
- (c) **Tungsten alloys** as promising candidates for so-called gas-cooled **divertors**, which are components loaded by up to **10 MW/m²** and operated at **700-1300°C**.*

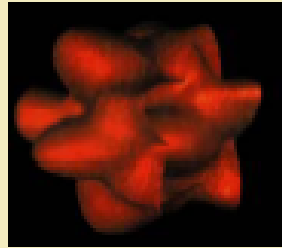
The KEY SYNERGETIC between
Multiscale Modeling and Experiments: *this is the “good highway”*



Space scales in materials and living systems

Increasing Physical Scale	Device and Material Systems		Biotechnical Systems	
	Nanocomposites	Opto-Electronics	Biomolecular	Cardiovascular
	 Windshield Coating (2 m)	 Solid-State Lamp (1 m)	 Bio-Chip (10 μm)	 Patient Imaging (1 m)
	 Cluster (1 μm)	 Bulb (1 cm)	 Multiprotein Assembly (10–50 nm)	 Artery Flow (1 cm)
	 Interface Zone (100 nm)	 LED (1 μm)	 Protein Structure (2–5 nm)	 Artery Walls (1 mm)
	 Interface/Atom (1 Å)	 Atomic Interactions (1 nm)	 Active Site (0.5 nm)	 Cells (10 μm)

Full-Scale, High-Fidelity Simulation Codes

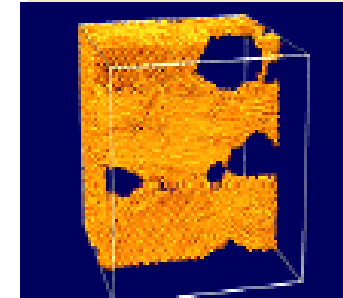
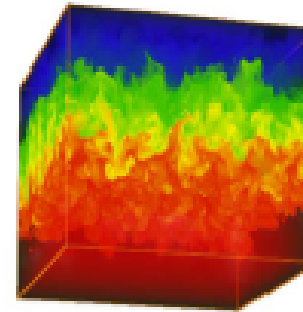


- 3D simulations
- High resolution
- Detailed physics
- Validation
- Parallel computing
- Scalable algorithms
- Mesh generation
- Visualization

Sub-grid Models / Zonal Physics

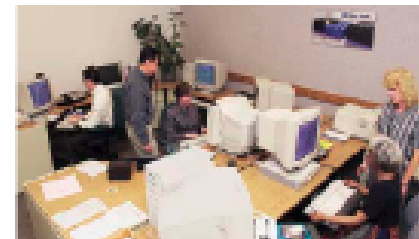
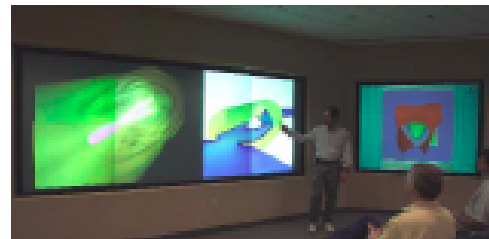
Turbulence

Materials Models



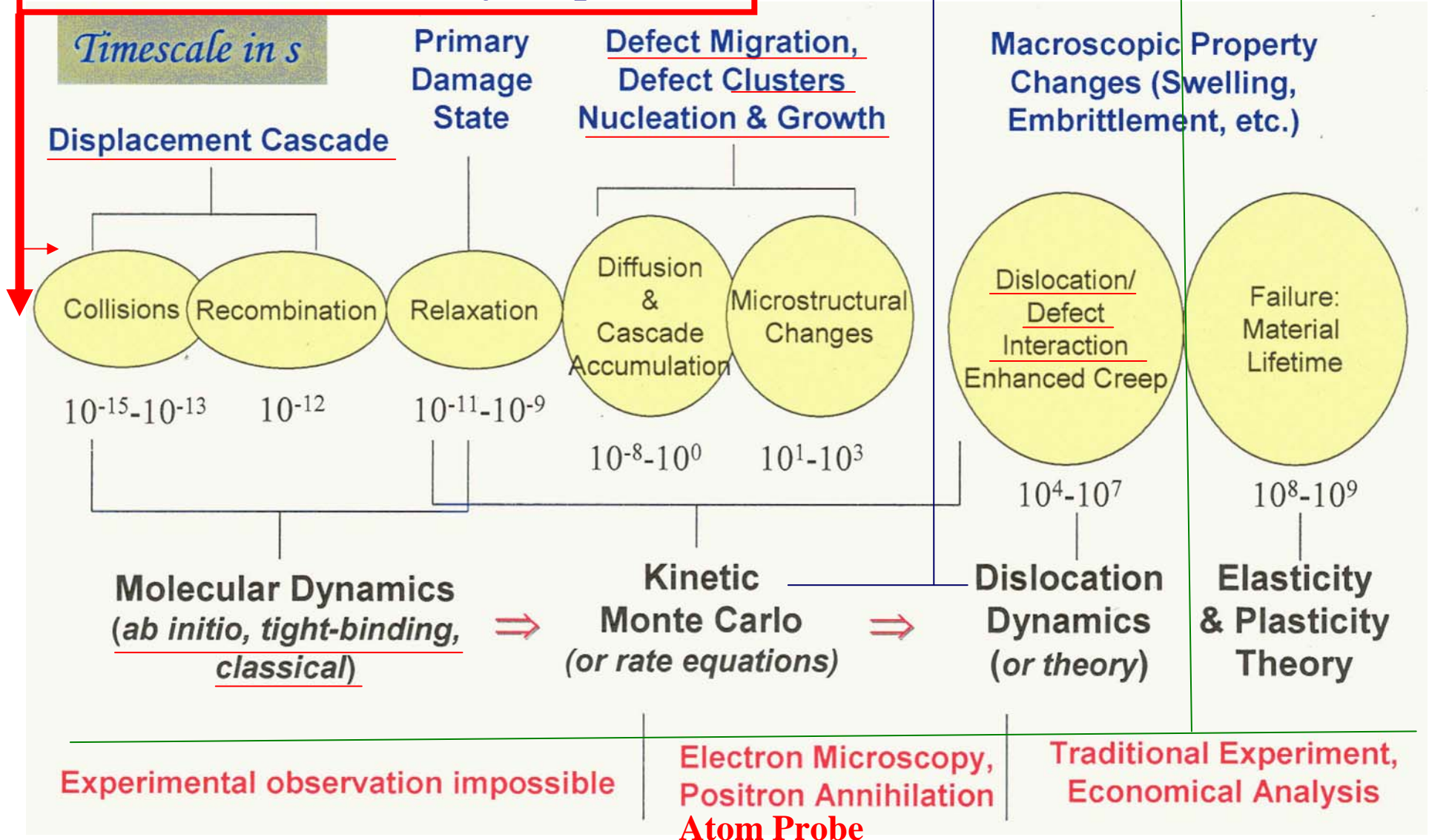
- Direct numerical simulations
- Predictive physics models
- First principle approaches

Advanced visualization facilities and LC's hotline are part of the "total simulation environment"



Mechanisms in Neutron Damage: **Modeling** and **Diagnosis**

Nuclear Reaction: *the first process*



Multiscale Modeling Approach

Quantitative computational materials science stands on two legs:

- Quantum Mechanics
- Thermodynamics

Usually requirements are beyond the Quantum Mechanics *ab initio* capabilities,

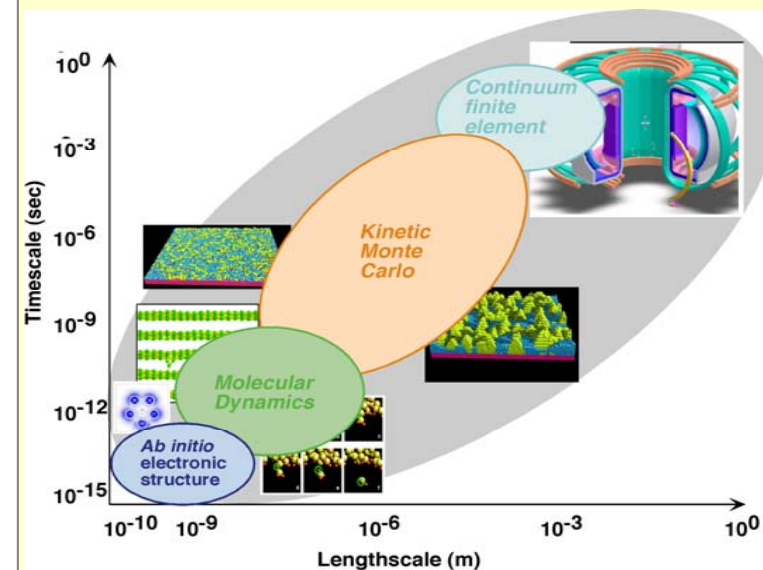


Approximations are used:

Multiscale Modeling is the path to follow

Usual approximations used in Mat Sci

- *Ab initio* for electronic structure
- Atomic potentials for MD/MC
- kMC, for time evolution
- Phase Field Method for microstructure evolution
- Continuum mechanics for mechanical response



Multiscale modeling

MULTISCALE MODELLING: COMPUTACIONAL



Atomistic Scale:

Working Area of DENIM

Pure Quantum-Mechanics Methods (“ab initio”)

Quantum-Mechanics Methods ***“Tight Binding”***

(DENIM code development)

Classical Molecular Dynamics (DENIM code development)

Microscopic Scale:

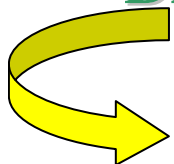
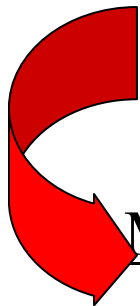
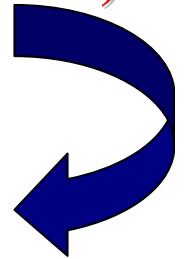
Rate Theory (different approaches)

Kinetic MonteCarlo (different solutions with/without lattice, DENIM code development PARALLEL)

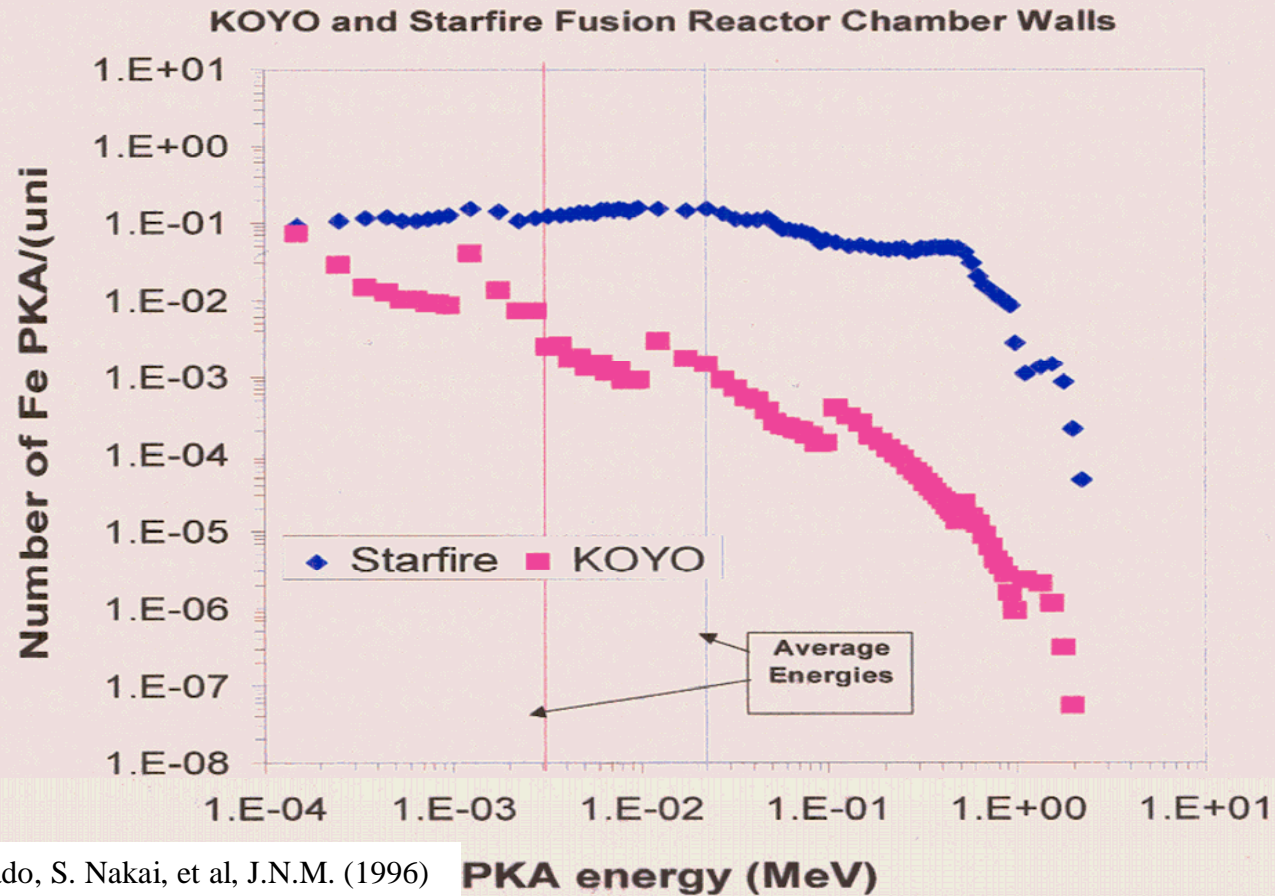
Mesoscopic Scale:

Dislocation Dynamics (present collaboration with LLNL/UCLA)

Macroscopic: Finite Elements



PKA Energy Spectra



J.M. Perlado, S. Nakai, et al, J.N.M. (1996)

PKA energy (MeV)

14th ANS Topical Meeting on the Technology of Fusion Energy, October 15-19, 2000, Park City, Utah

Ab Initio Simulations of Matter

The problem in its basic and fundamental form from *Quantum Mechanics* considers N nuclei with coordinates $R_1, \dots, R_n \equiv \mathbf{R}$, and momenta $P_1, \dots, P_n \equiv \mathbf{P}$, and N_e electrons with coordinates $r_1, \dots, r_n \equiv \mathbf{r}$, and momenta $p_1, \dots, p_n \equiv \mathbf{p}$ and spin variables $s_1, \dots, s_n \equiv \mathbf{s}$ with Hamiltonian

$$H = \sum_{I=1}^N \frac{\mathbf{P}_I^2}{2M_I} + \sum_{i=1}^{N_e} \frac{\mathbf{p}_i^2}{2m} + \sum_{i>j} \frac{e^2}{|\mathbf{r}_i - \mathbf{r}_j|} + \sum_{I>J} \frac{Z_I Z_J e^2}{|\mathbf{R}_I - \mathbf{R}_J|} - \sum_{i,I} \frac{Z_I e^2}{|\mathbf{R}_I - \mathbf{r}_i|}$$
$$\equiv T_N + T_e + V_{ee}(\mathbf{r}) + V_{NN}(\mathbf{R}) + V_{eN}(\mathbf{r}, \mathbf{R})$$

We want to obtain eigenfunctions and eigenvalues of Schrödinger's:

$$[T_N + T_e + V_{ee}(\mathbf{r}) + V_{NN}(\mathbf{R}) + V_{eN}(\mathbf{r}, \mathbf{R})] \Psi(\mathbf{x}, \mathbf{R}) = E\Psi(\mathbf{x}, \mathbf{R})$$

with nuclear and electron kinetic energies, and electron-electron, nuclear-nuclear, and electron-nuclear interactions operators.

AN EXACT SOLUTION OF THIS EQUATION IS EXTREMELY DIFFICULT !

Ab Initio Simulations of Matter: *Born-Oppenheimer*

This approximation consists in the recognition that there is a strong separation between the times scales of the nuclear and electronic motion, since the electrons are lighter than nuclei (three orders of magnitude), then:

$$\Psi(\mathbf{x}, \mathbf{R}) = \phi(\mathbf{x}, \mathbf{R})\chi(\mathbf{R})$$

with electronic and nuclear wave functions respectively, in which the electronic wave function depends parametrically on the nuclear position.

$$\begin{aligned} T_N \phi(\mathbf{x}, \mathbf{R})\chi(\mathbf{R}) \\ = \frac{\hbar^2}{2} \sum_{I=1}^N \frac{1}{M_I} [\phi(\mathbf{x}, \mathbf{R}) \nabla_I^2 \chi(\mathbf{R}) + \chi(\mathbf{R}) \nabla_I^2 \phi(\mathbf{x}, \mathbf{R}) + 2 \nabla_I \phi(\mathbf{x}, \mathbf{R}) \cdot \nabla_I \chi(\mathbf{R})] \end{aligned}$$

The Born-Oppenheimer approximation indicates that $\nabla_I \phi(\mathbf{x}, \mathbf{R})$ can be neglected.

The reason is that the nuclear wave function $\chi(\mathbf{R})$ is more localized than the electronic wave function; in consequence, $\nabla_I \chi \gg \nabla_I \phi$, and operating:

$$\frac{[T_e + V_{ee}(\mathbf{r}) + V_{eN}(\mathbf{r}, \mathbf{R})] \phi(\mathbf{x}, \mathbf{R})}{\phi(\mathbf{x}, \mathbf{R})} = E - \frac{[T_N + V_{NN}(\mathbf{R})] \chi(\mathbf{R})}{\chi(\mathbf{R})}$$

DENSITY FUNCTIONAL THEORY from Hohenberg-Kohn theorem

1998 Nobel Prize in Chemistry to Walter Kohn and John Pople

The ground state energy $\varepsilon_0(\mathbf{R})$ at a given nuclear configuration, \mathbf{R} , is obtained by minimizing a certain functional, $\varepsilon(\mathbf{n})$, which depends on the electron density. That functional assumes its minimum at the ground state electron density.

$$n(\mathbf{r}) = \sum_{s_1, s_2, \dots, s_{N_e}} \int d\mathbf{r}_2 \cdots d\mathbf{r}_{N_e} |\varphi_0(\mathbf{r}, s_1, \mathbf{r}_2, s_2, \dots, \mathbf{r}_{N_e}, s_{N_e})|^2$$

Equation 3

[Hohenberg and Kohn, Phys.Rev. **136** (1964) 864]:

A convenient form of this functional is given by the scheme of

KOHN-SHAM where a doubly occupied single-states, $\psi_i(\mathbf{R})$, $i=1, \dots, N_e/2$, each containing an spin up and down is introduced. [W. Kohn and L. J. Sham, Phys Rev. **140** (1965) 1133]

The density and functional are expressed:

$$\varepsilon[\{\psi_i\}] = -\frac{\hbar^2}{2m} \sum_i \langle \psi_i | \nabla^2 | \psi_i \rangle + \frac{e^2}{2} \int d\mathbf{r} d\mathbf{r}' \frac{n(\mathbf{r})n(\mathbf{r}')}{|\mathbf{r} - \mathbf{r}'|} + \varepsilon_{xc}[n] + \int d\mathbf{r} n(\mathbf{r})V_{en}(\mathbf{r}, \mathbf{R})$$

Quantum kinetic energy

Direct Coulomb term from Hartree-Fock theory

Exact exchange and correlation

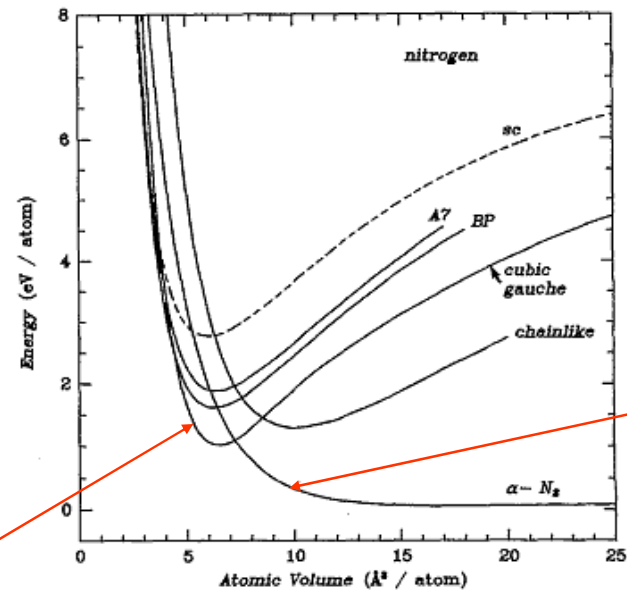
Interaction of electron density with external potentials

A new phase of Nitrogen

- Published in Nature.
Dense, metastable semiconductor
- Predicted by theory
~10 years ago!

Mailhiot, et al 1992

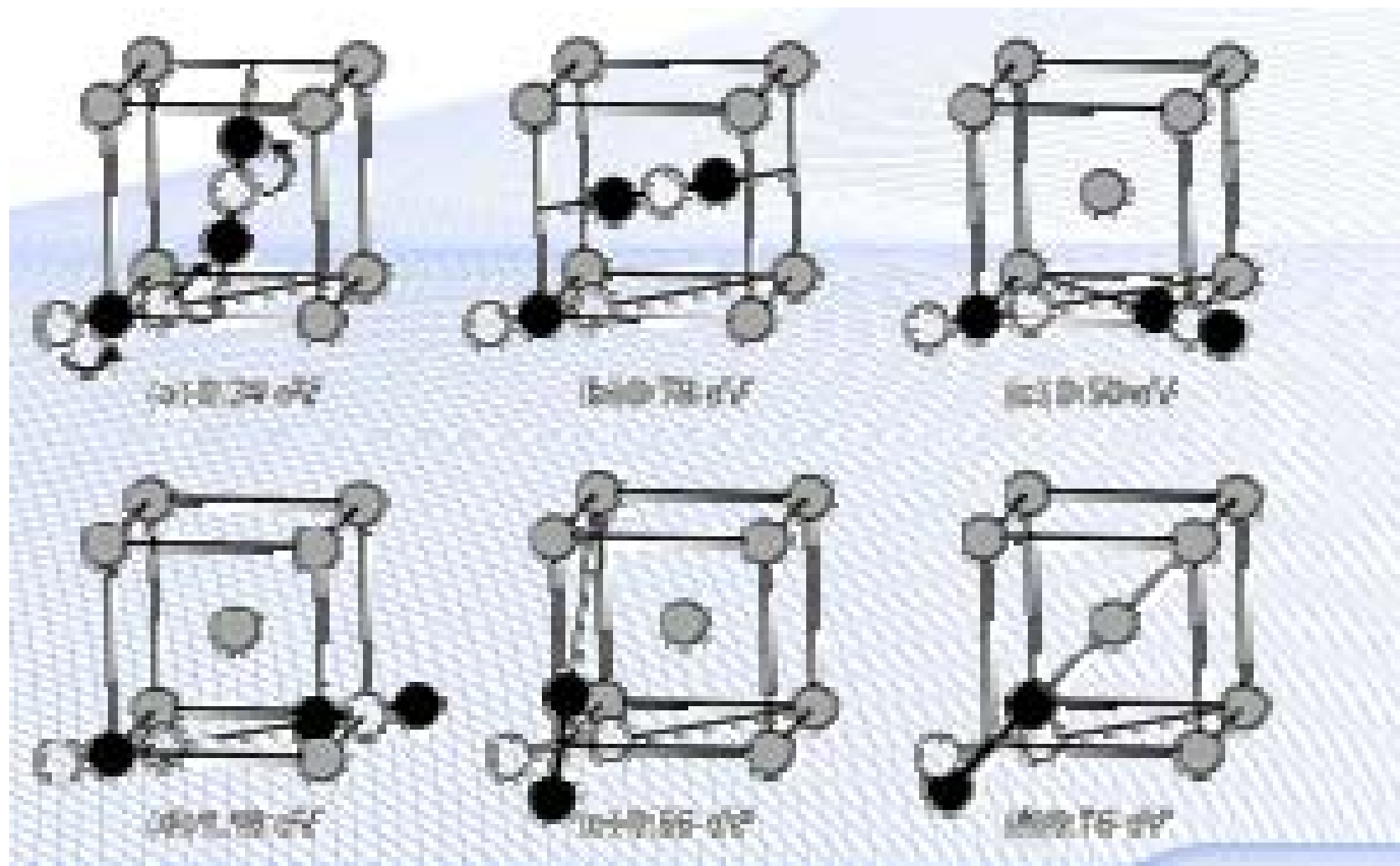
“Cubic Gauche”
Polymeric form with
3 coordination

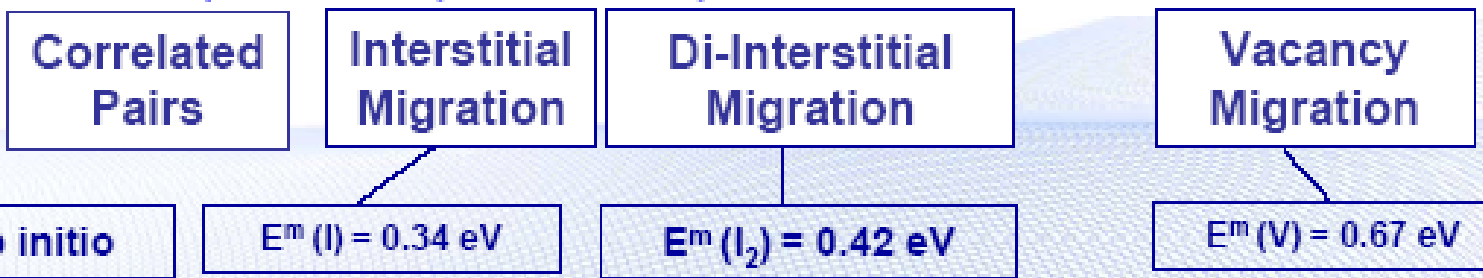
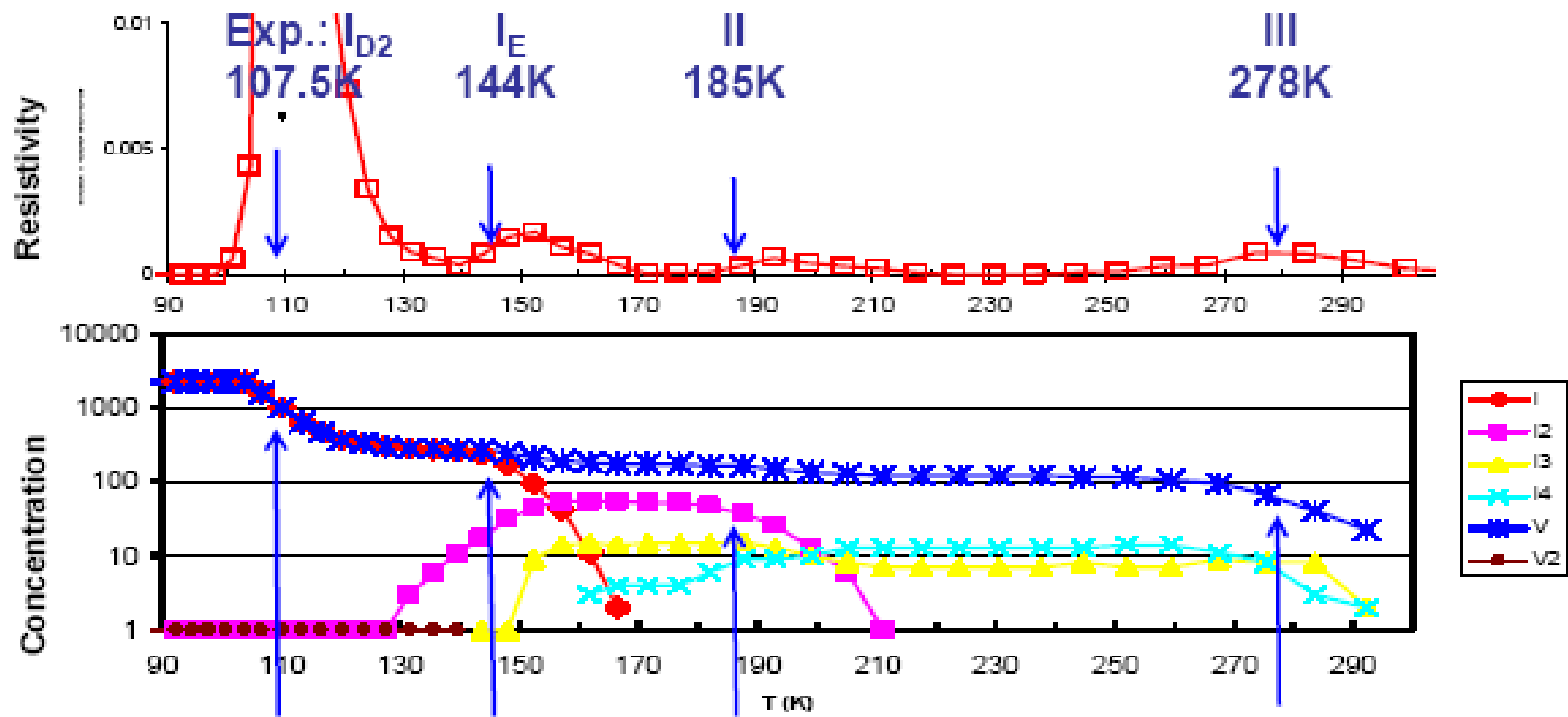


Molecular
form

FIG. 3. *Polymeric phases of nitrogen.* Calculated total energy per atom for the threefold-coordinated arsenic (A7), black-phosphorus (BP), and cubic gauche (cg) phases of nitrogen, and for a twofold-coordinated chainlike (ch) phase of nitrogen, as a function of atomic volume. A kinetic energy cutoff of $E_{\text{cutoff}} = 80$ Ry was used to calculate the total energy for all the structures. The number of k points used for the calculations was A7 (28), BP (16), cg (18), and ch (16). The zero of energy corresponds to the minimum energy of the diatomic α -N₂ ($Pa\bar{3}$) phase, which is discussed in Sec. III D. The simple-cubic (sc, dashed curve) phase is included here for comparison.

Ab initio Calculation of Migration Energy of $\langle 110 \rangle$ SIA in Fe





S. Takaki, J. Fuss, H. Kugler, U. Dedek and H. Shultz, *Radiat. Effects* 79 (1983) 87-122

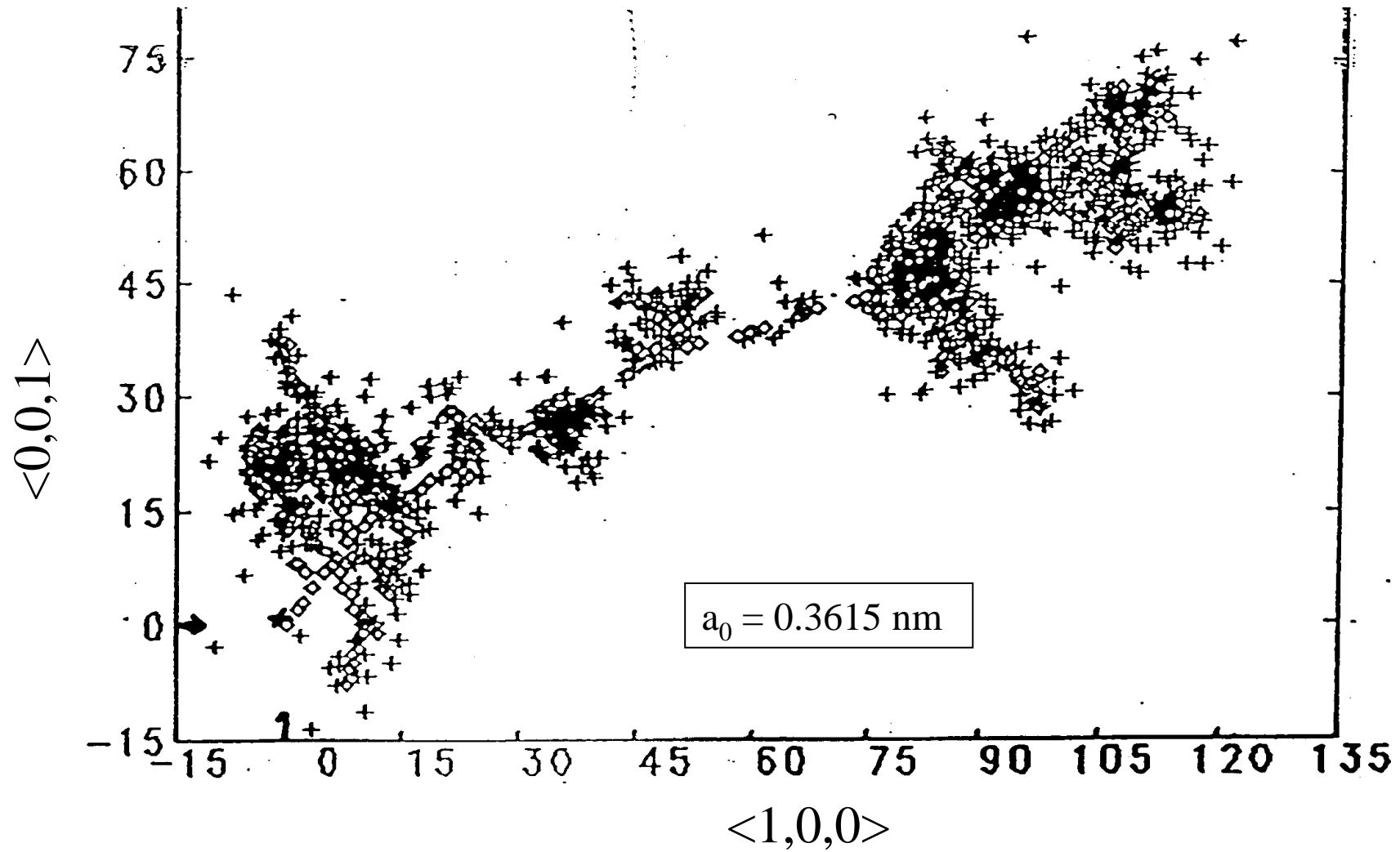
C.C. Fu, J. Dalla Torre, F. Willaime, J.L. Bocquet, A. Barbu in *Nature Materials* 4, 68 (2005)

Binary Collision Approximation

- Interatomic Potentials:
- Screened Coulomb Potentials:
 - Moliere, Firsov.
- Universal Potential from Ziegler, Biersack *and* Littmark (*ZBL*) using Hartree-Fock-Slater (*HFS*) atomic charge distributions:

$$\phi_u = \sum_{i=1}^4 c_i \exp\left(-d_i \frac{r}{a_u}\right)$$

$$a_u = 0.8853a_0 (Z_1^{0.23} + Z_2^{0.23})^{-1}$$



Cascade formation by MARLOWE 200 keV Cu in Cu / J.M. Perlado, J. Sanz et al JNM (1992)

A part of study for comparison of defect structures between Fusion and Spallation Neutron Spectra

MOLECULAR DYNAMICS

- Integration of the Newton's equations of motion for all the atoms in a computational cell \Rightarrow Trajectories
- Interaction between the particles through an empirical potential.....for a conservative potential:

$$\vec{F}_i = -\nabla V(\vec{r})$$
$$\frac{d^2 \vec{r}}{dt^2} = \frac{\vec{F}_i}{m_i}$$

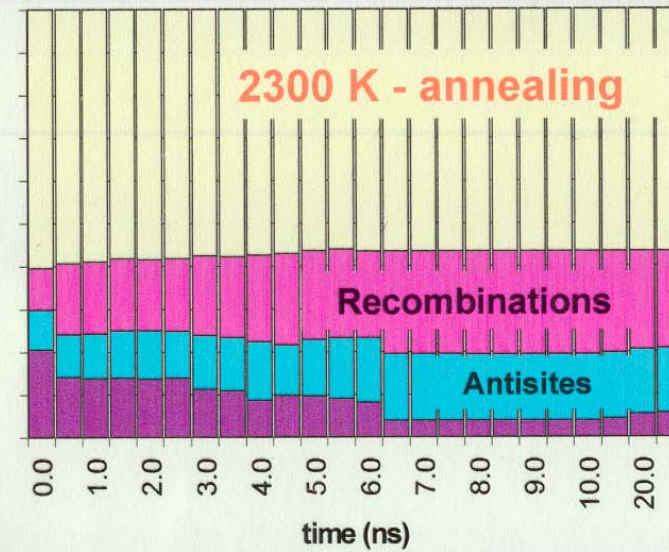
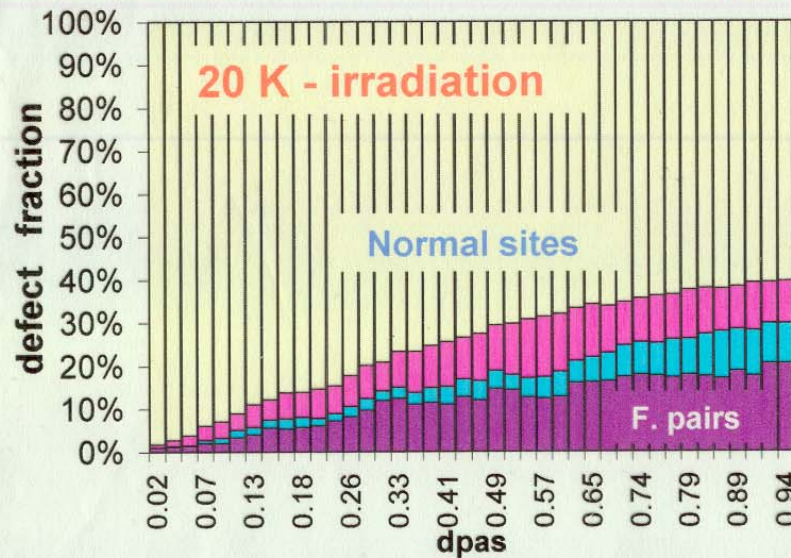
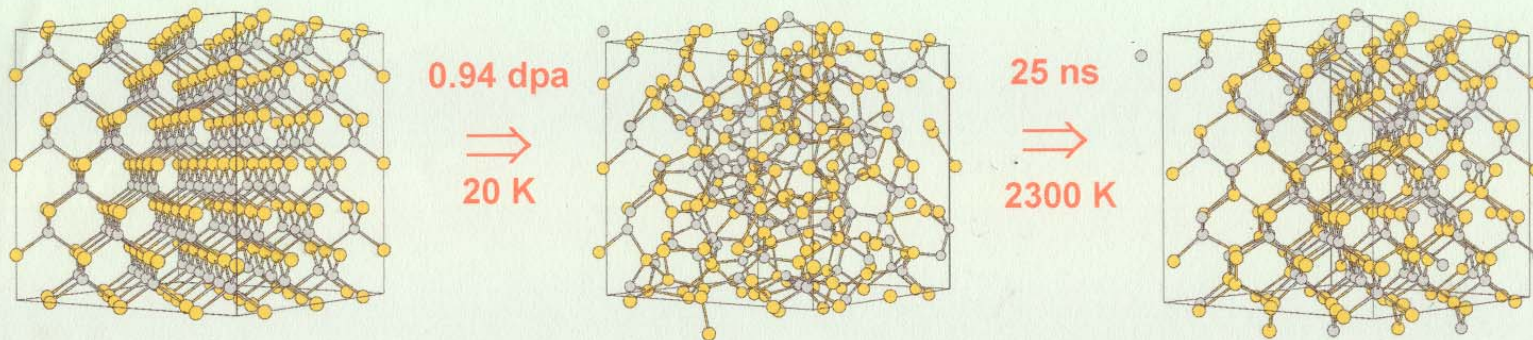
MOLECULAR DYNAMICS

Interatomic Potentials

Some more used:

- *Isotropic*
 - *Embedded Atom Model (EAM) and modifications (Metals)*
 - *Finnis- Sinclair method (alternative to EAM)*
 - *Johnson-Oh (EAM for BCC structures)*
- *Non-isotropic, useful for covalent bonding (highly directional)*
 - *Stillinger-Weber*
 - *Tersoff*
 - *Pearson (Born-Meyer + Axilrod-Teller)*

Summary



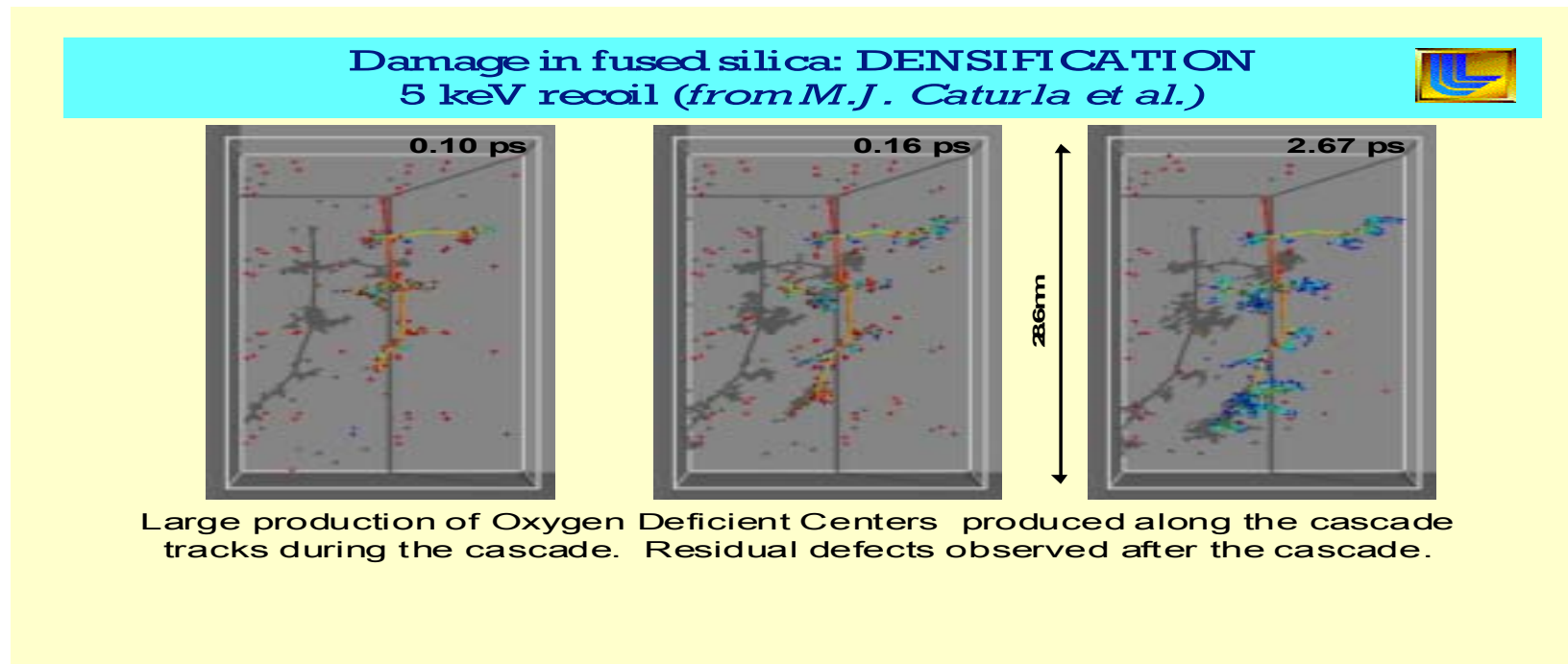
Molecular dynamics simulation of irradiation-induced amorphization in cubic silicon carbide - 21

Consequences of the Interaction of Radiation in Materials

Electrons = simple *Frenkel* pairs

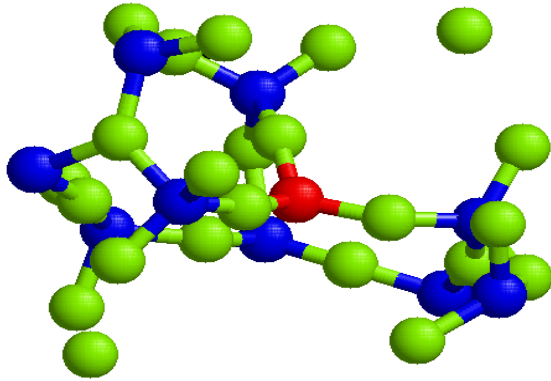
Ions/Neutrons/Gammas = *Atomic displacement cascades*

- point structure defects:
- vacancies, interstitials
- clusters of vacancies, clusters of interstitials
- segregation of alloying elements

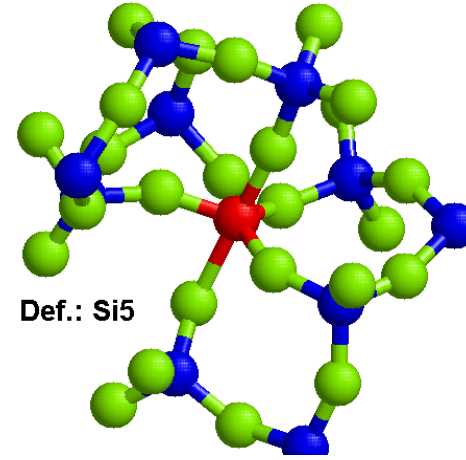


Characterization of defects (Si-O 2.15 Å)

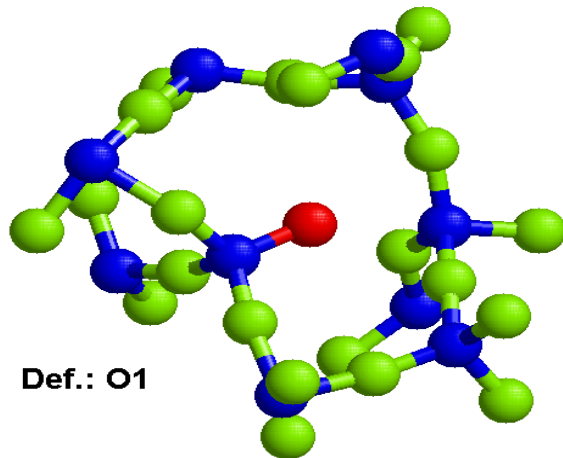
Good agreement with experiments



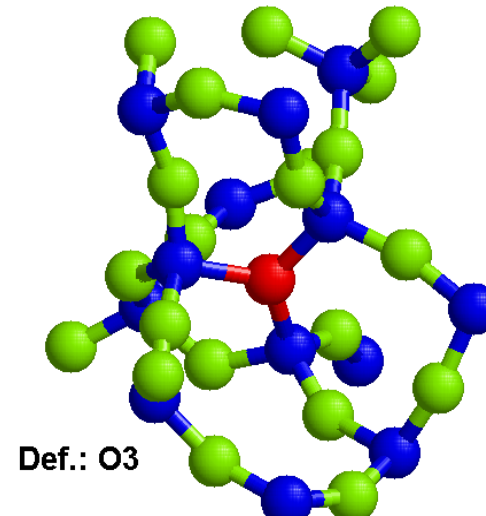
Def.: Si3



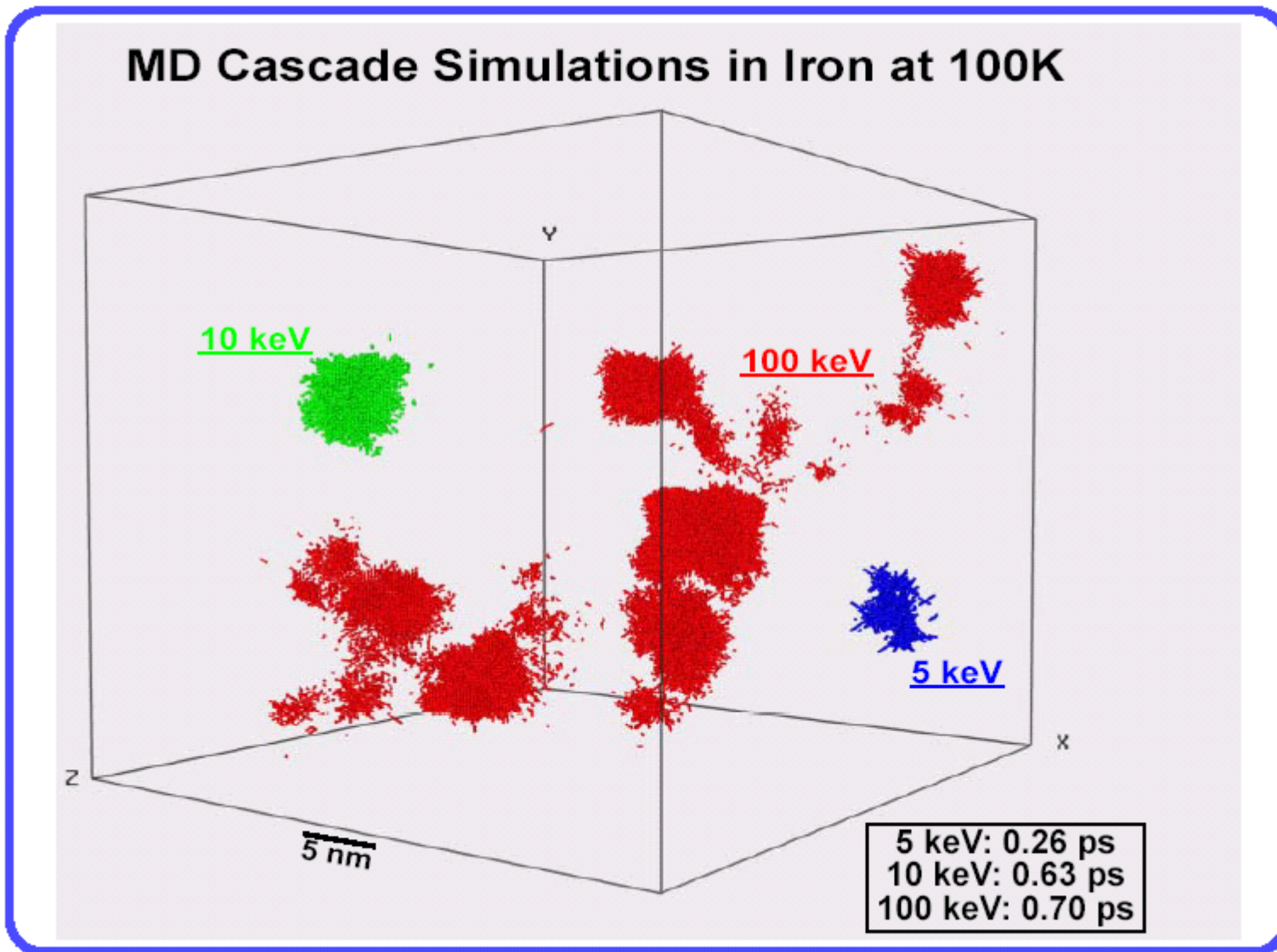
Def.: Si5



Def.: O1



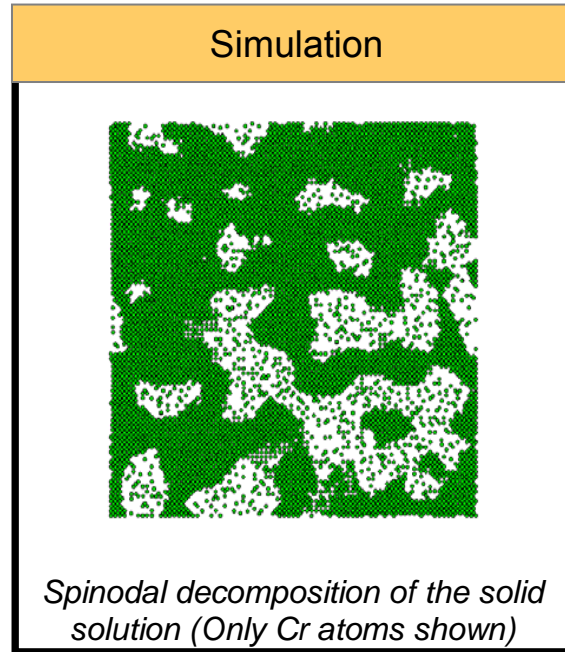
Def.: O3



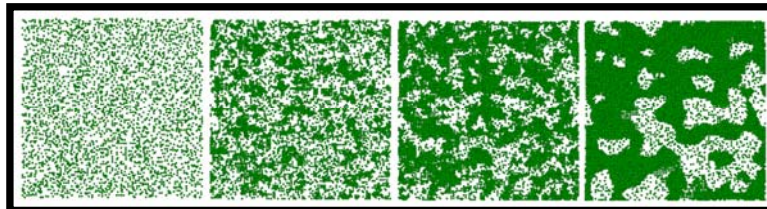
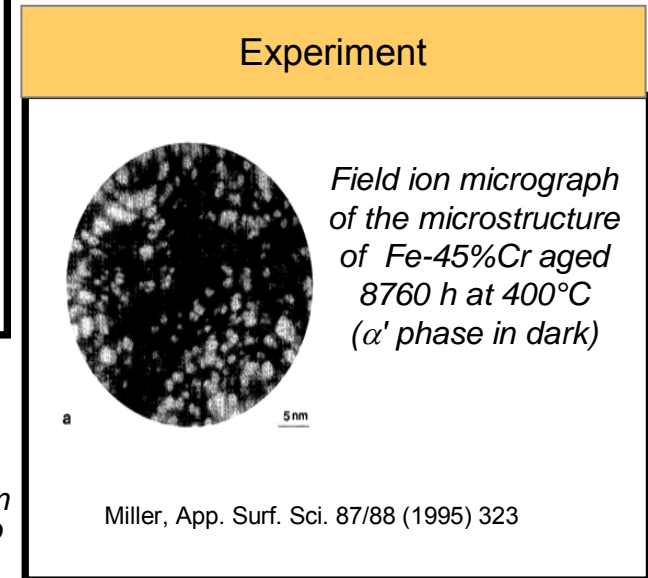
Phase separation in FeCr alloys in the solid solution

Combined MC/MD calculations applied to study phase separation thermodynamics in FeCr alloys

- First qualitative comparison with experiments: α' precipitation is observed in thermally-aged alloys



LLNL simulations show the formation of a Cr-rich α' phase in FeCr alloys
 $T \sim 750K$

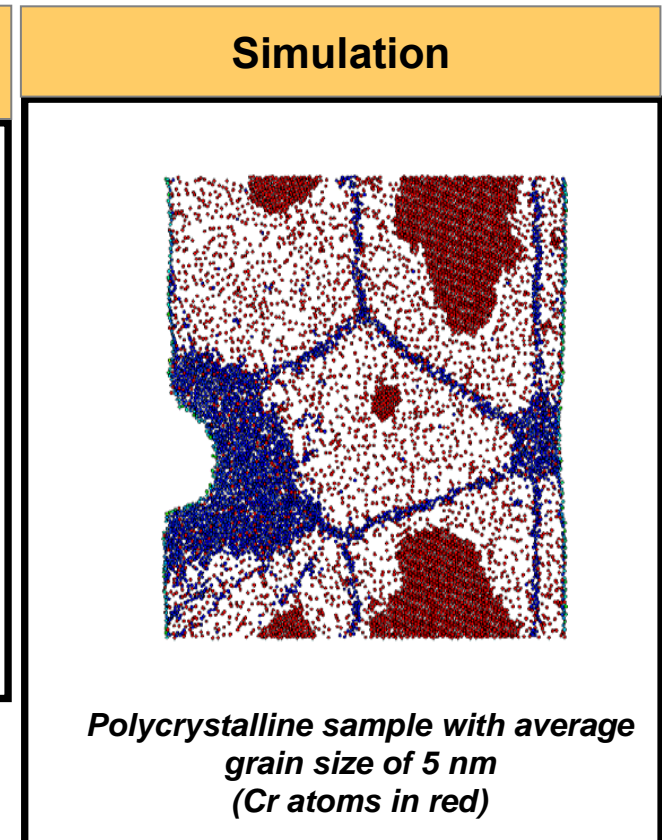
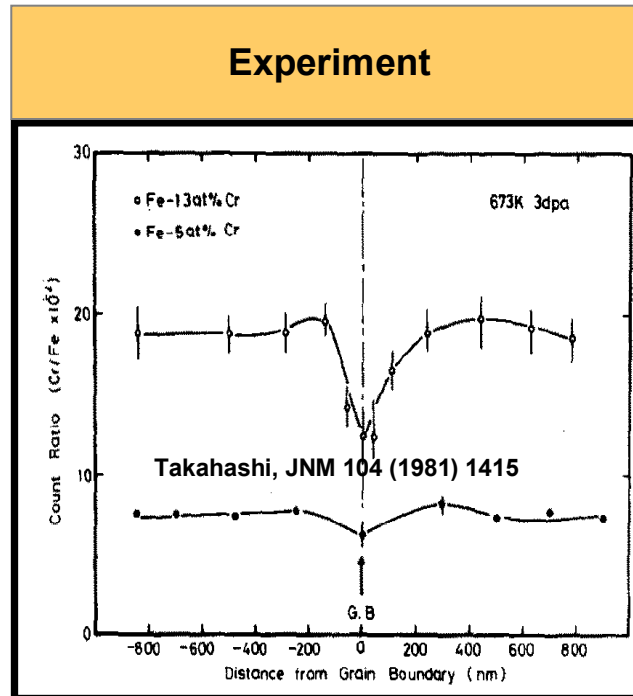


Continuous increase of composition differences from Cr concentrations of 50% to the terminal solution values of 12% for α and 99% for α'

Science Impact: Atomistic simulations agree with atomic scale experiments

Heterogeneous precipitation in FeCr alloys

- Approaches capture the thermodynamics of the FeCr system
- We are able to describe the way in which Cr precipitates in the α' phase in the presence of heterogeneities (grain boundaries, cracks, surfaces, dislocations, etc.)



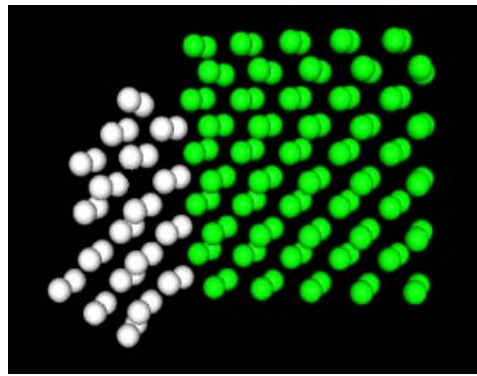
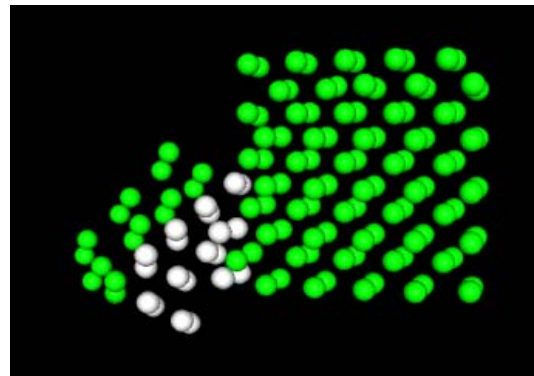
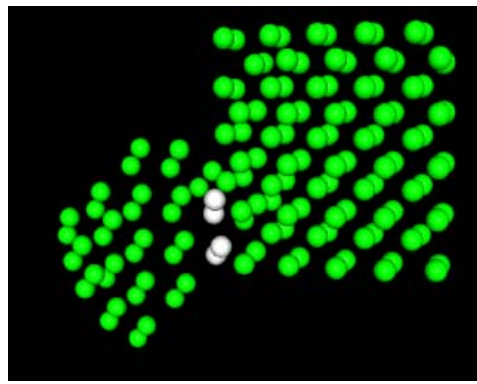
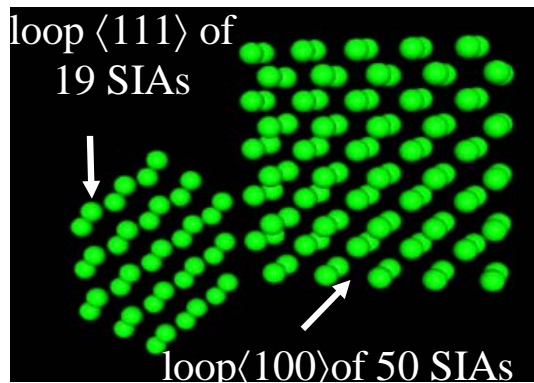
Science Impact - Surprising effect
Cr does not precipitate at boundaries

α' precipitates are at the interior of the grains, avoiding contact with the GB network

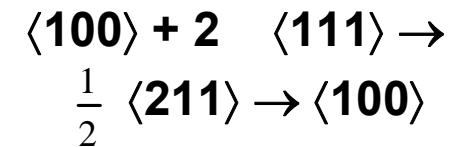
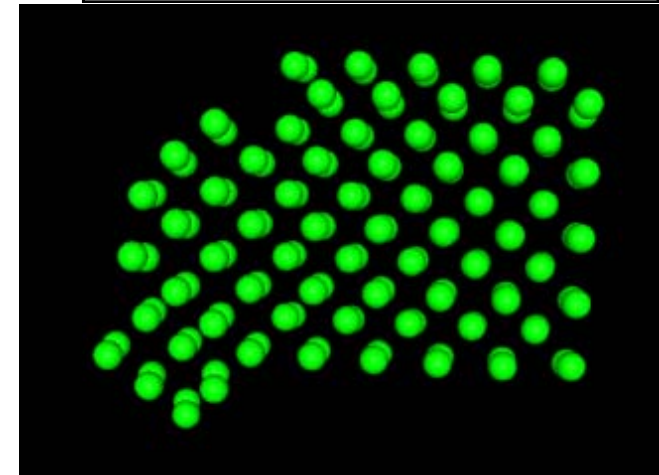
A. Caro, M. Caro, P. Klaver, E. M. Lopasso, and B. Sadigh, "Computational modeling of alloys at the atomic scale: from ab-initio and thermodynamics to radiation induced heterogeneous precipitation", to be published in JOM, Feb 07

Mechanism of growing $\langle 100 \rangle$ dislocation loops in Fe

- Even metastables with respect to $\frac{1}{2} \langle 111 \rangle$, loops $\langle 100 \rangle$ growth absorbing loops $\frac{1}{2} \langle 111 \rangle$ smaller



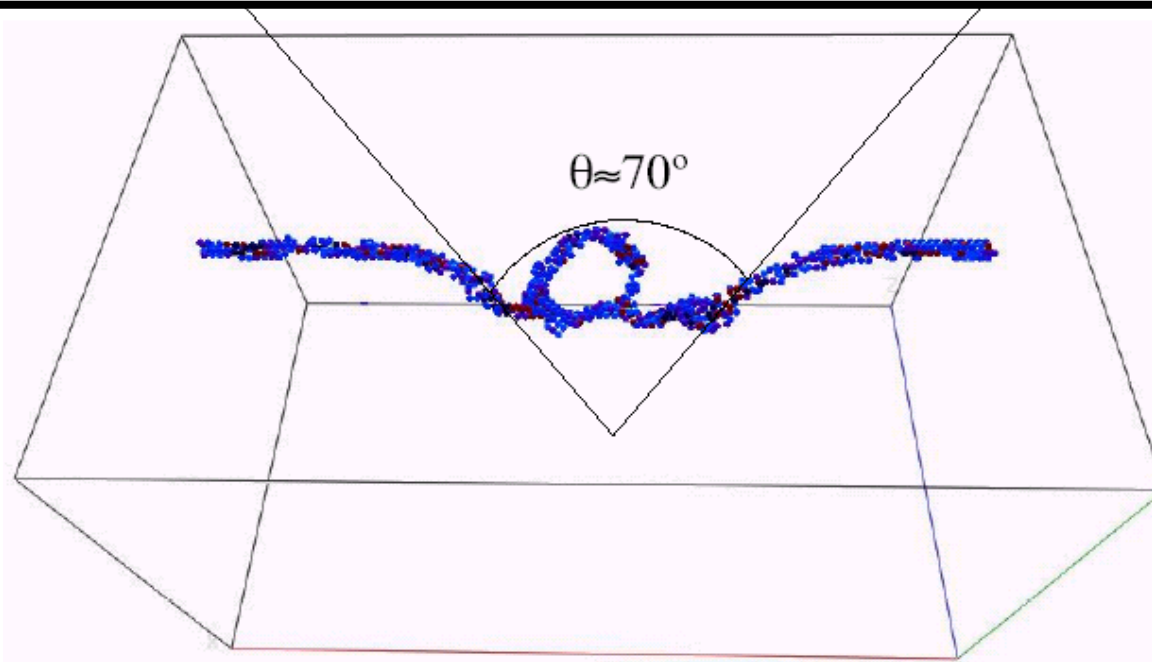
J. Marian Thesis (UPM) and PRB 65 (2002) 144102/1-11



MOLECULAR DYNAMICS: predicting behaviour of simple materials

New process of defect formation.

Last snapshot before the dislocation breaks through the obstacle, leaving a [100] loop behind and two heavily-curved spirals along the dislocation line. The critical angle is $\theta=70^\circ$, necessary to estimate the obstacle strength α . **Stress computed using Orowan theory is 590 Mpa; that is an error with experiments of only 50 %.** (J. Marian, B. Wirth, B. Odette, R. Schaublin,, J.M. Perlado, J. Nuclear Materials (2003))

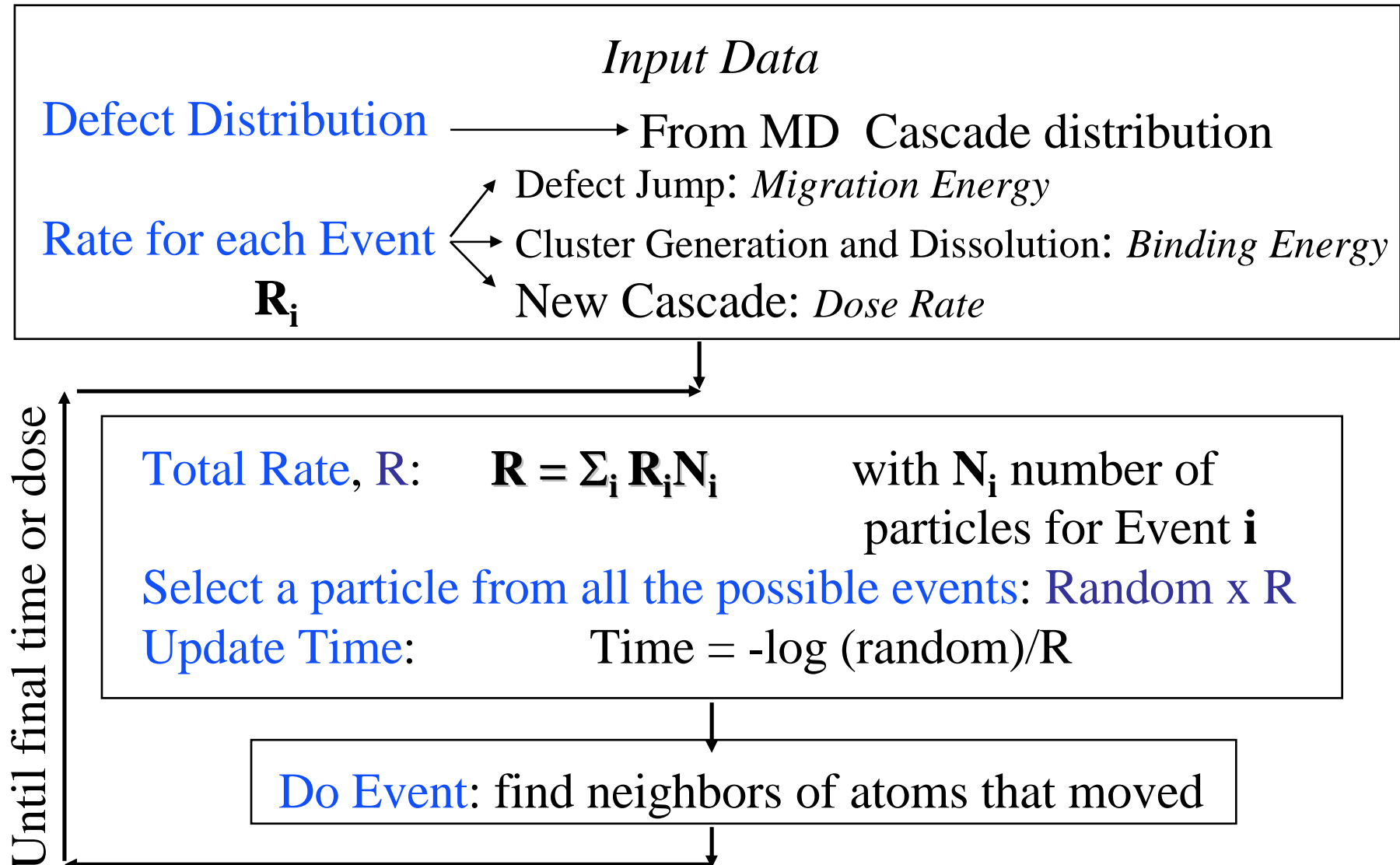


$$\theta \approx 70^\circ$$

$$\cos\left(\frac{\theta}{2}\right) = \alpha \approx 0.8$$

**Molecular
Dynamics:
Macroscopic
Application
Defining
Stress-Strain
curve**

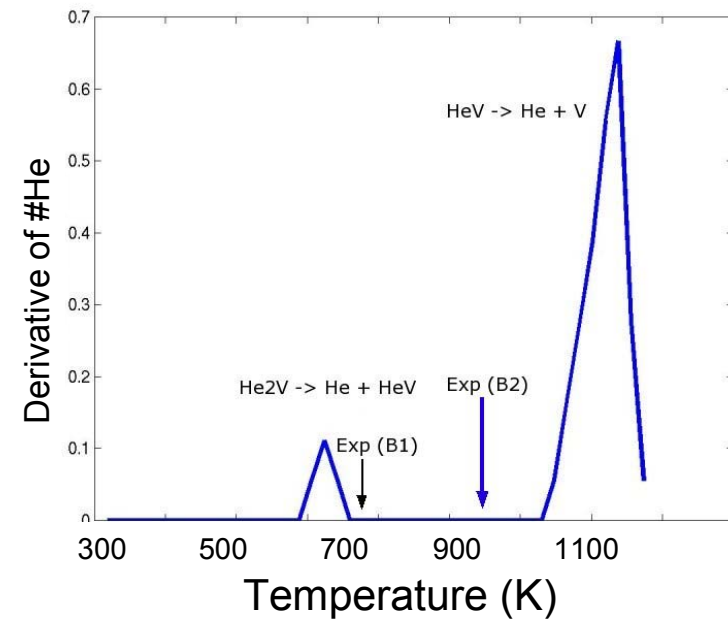
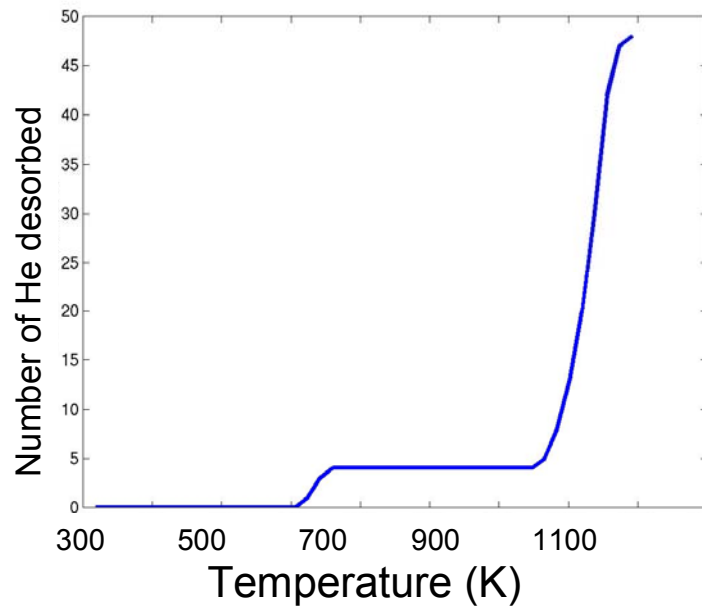
Kinetic Monte Carlo Simulation Methodology



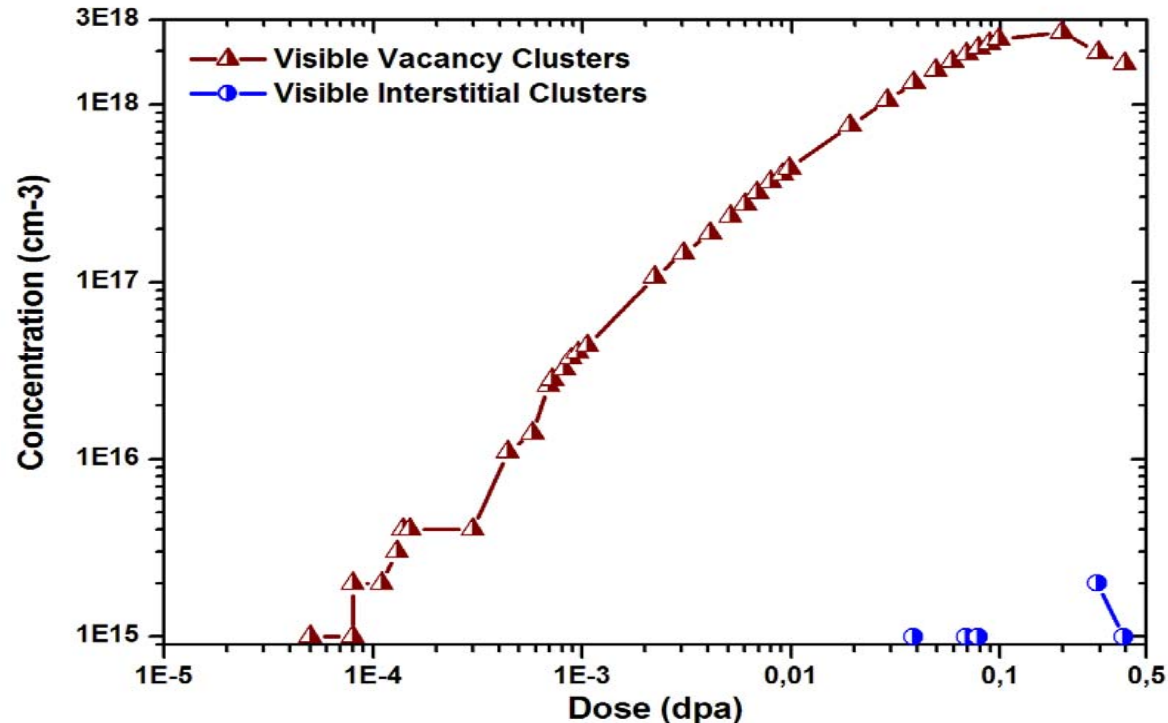
Results of OKMC simulations under the conditions of Edwards et. al

- He 400 eV -> Ni – damage distribution obtained with SRIM
- Implantation at 300K – defects followed until steady state is reached
- Annealing and measurement of desorption of He from 300K until 1200K
- Ramp rate 18.4 K/s

Two peaks are also obtained from the simulations corresponding to the dissociation of He_2V and HeV



Visible defect concentration at 600K in Zr (Arevalo, Caturla, Perlado, Nucl.Inst.Meth (2006))



Visible:
clusters with
more than 50
defects ~ 2nm

According to the model at 600K most of the defects are Vacancy type
The concentration of self-interstitials is very low due to the 1D migration

Experiments

Y. Dai,

M. Victoria
(MRS)

This is a clear example of successful use of KMC in comparison with experiments

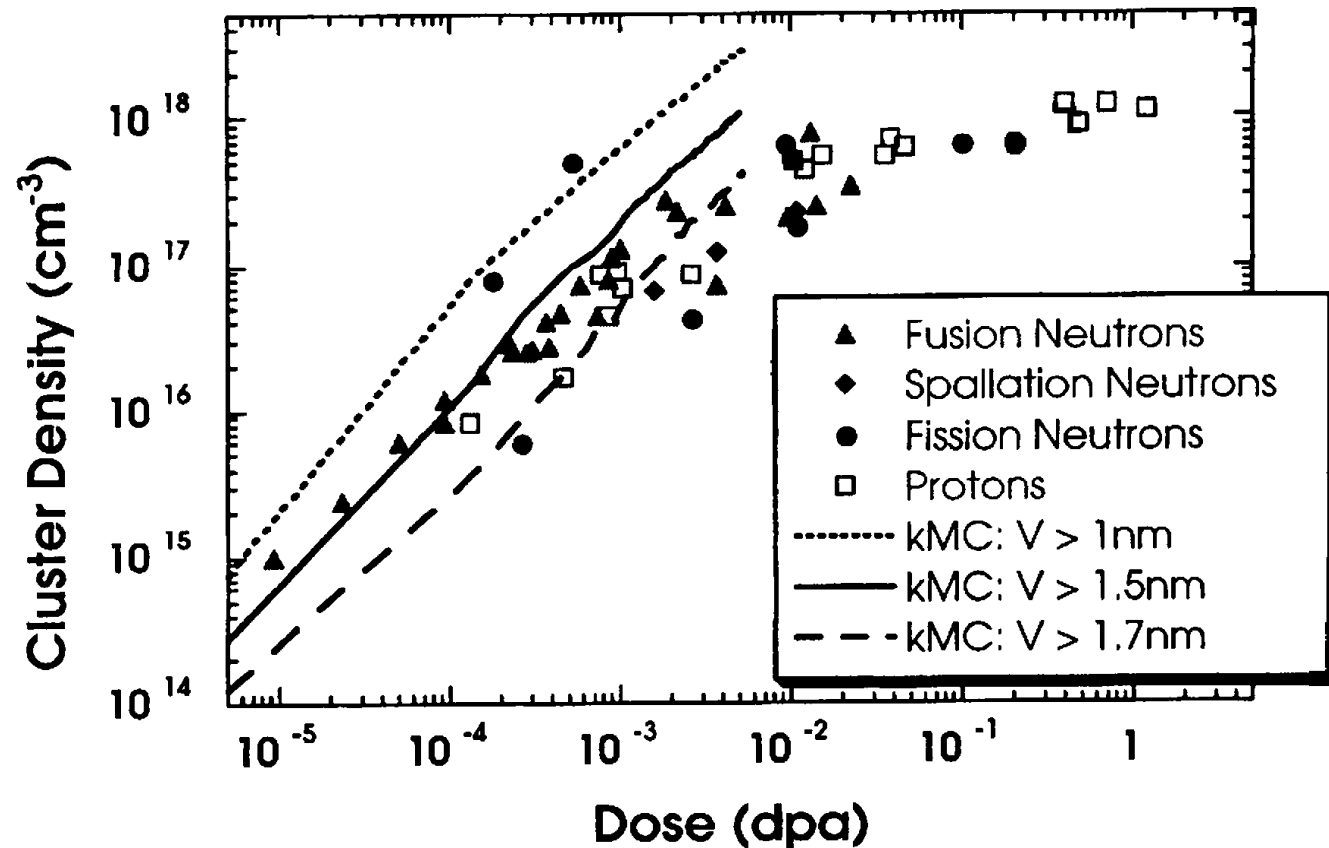


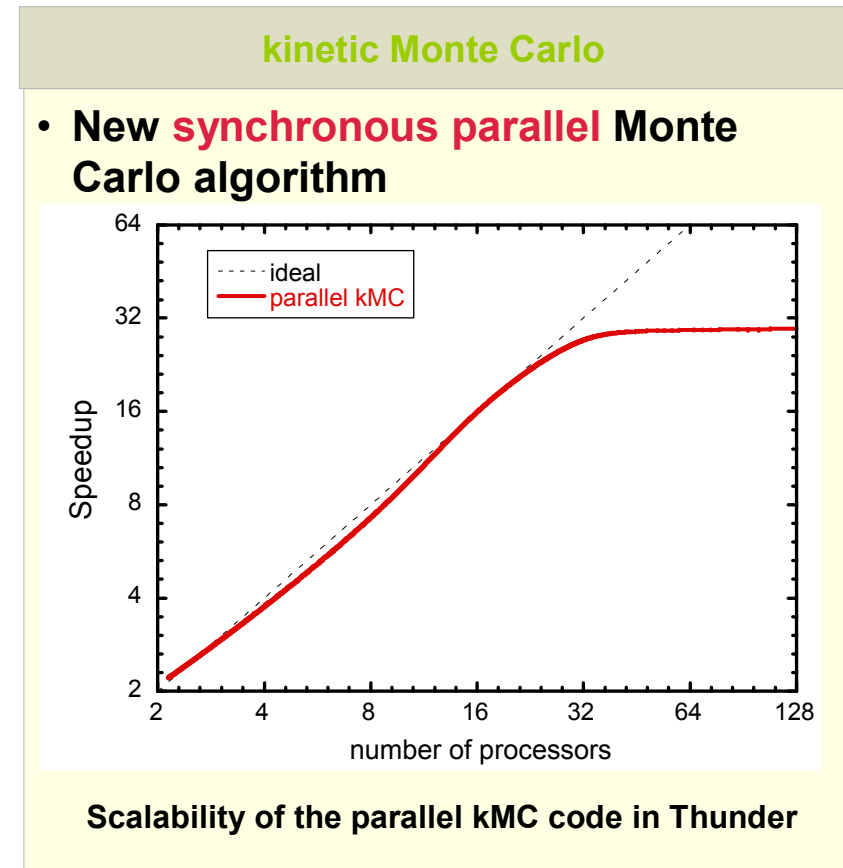
Fig. 7. 'Visible' cluster density for Cu. Comparison to experimental results under different irradiation conditions. Three cluster sizes are considered as 'visible' in the simulations: vacancy clusters larger than 1, 1.5 and 1.7 nm.

M.J. Caturla, N. Soneda, E. Alonso, B. Wirth, T. Díaz de la Rubia, J.M. Perlado, JNM 276 (2000) 13-21

New massively-parallel Monte Carlo method for fast microstructural kinetic evolution calculations

- Conditions in Gen-IV, ABR, reactors require exploring long timescales (high accumulated doses) → current state-of-the-art cannot cover them
- We have developed a novel algorithm to do kinetic Monte Carlo in parallel
- The method is synchronous, which facilitates its implementation compared to traditional asynchronous methods
- Science impact:
 - Microstructural evolution due to irradiation damage up to ~ 10 dpas (best available codes can only reach up to ~1 dpa)
 - Connection with defect property calculations done by H. Dogo and R. Till
- Irradiation damage groups in Europe and Japan have already expressed interest in this method

E. Martínez, J. Marian. M. Kalos, J.M. Perlado, *Journal of Computational Physics* (Jan 07)



Use of Lattice Kinetic Monte Carlo to track interstitial He, substitutional He and vacancies, in order to investigate initial stages of He bubble nucleation in bcc metals. It is found formation of He dimers and trimers

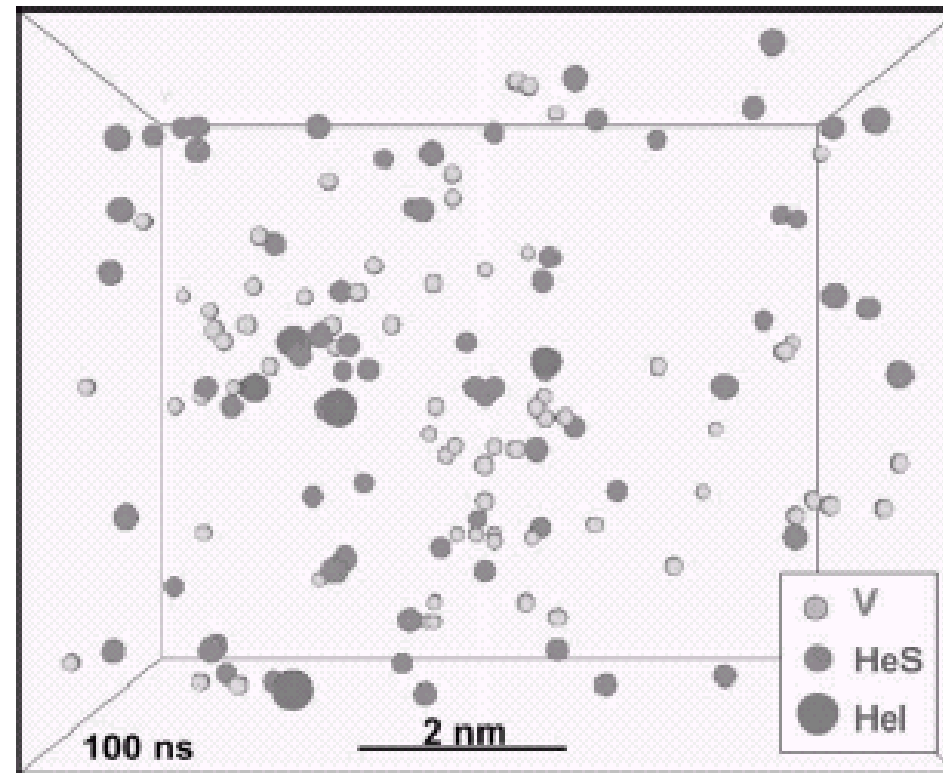


Fig. 7. Snapshot at 0.1 μ s from a LKMC run at 650 K. Only V, HeS and HeI sites are shown. Initial state ($t = 0 \mu$ s): V distribution from 20 keV cascade (aged), 0.05% residual V and 0.1% He (2/3 as HeS). Only 73 V and 5 HeI were left when the snapshot was taken.

A clear example of Multiscale Modeling in Radiation Damage using the different tools:

Multiscale Modelling of plastic flow localization in irradiated materials. T.Díaz de la Rubia et al., Nature Vol 406, 24 August 2000, 871-873

Stress-Strain curve simulation in irradiated Cu ($\rho_B = 8.24 \times 10^{21} \text{ m}^{-3}$) with uniform defect distribution with SFT spacing of 50 nm. Initial dislocation network $\rho_N = 10^{12} \text{ m}^{-2}$. Without irradiation yield at 37 MPa, and work hardening starts at early stage of deformation due to dislocation multiplication and forest interaction. If irradiation: i) if defects density along the line (ρ_D) is such that the spacing is 10 nm, $\rho_D \gg \rho_B$, a clear yield point followed by a yield drop is observed; ii) if spacing is 30 nm, comparable to that in the bulk the system yields at a slightly higher stress and a very diffuse yield drop appears. **GOOD AGREEMENT WITH EXPERIMENTS** that shows how the yield drop disappears when $\rho_D \approx \rho_B$.

In irradiated Pd the dose dependence of the yield stress obtained in DD simulations (with Frank sessile dislocation loops) has a slope of 0.35 with **EXCELLENT AGREEMENT WITH EXPERIMENTS** (see Khraishi, et al., Localized deformation and hardening in irradiated metals. 3D discrete dislocations dynamics simulations. *Acta Metall. Mater.*)

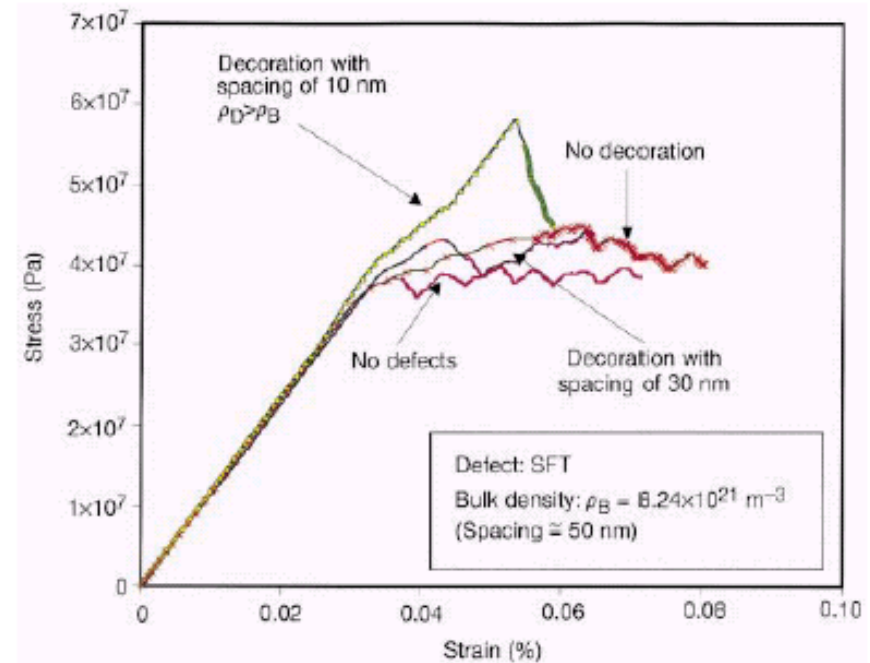


Figure 3 Dislocation dynamics (DD) results of stress–strain curves. Shown are the stress–strain curves obtained with our DD simulations for Cu irradiated to $\rho_B = 8.24 \times 10^{21} \text{ m}^{-3}$. Without irradiation the system yields at about 37 MPa. When the defect density along the line (ρ_D) is such that $\rho_D \gg \rho_B$, a clear yield point followed by a yield drop can be observed. However, when the average spacing between defects along the dislocation line is 30 nm, which is comparable to that in the bulk, the system yields at a slightly higher stress and only a very diffuse yield drop is apparent.

A clear example of Multiscale Modeling in Radiation Damage using the different tools:

Multiscale Modelling of plastic flow localization in irradiated materials. T.Díaz de la Rubia et al., Nature Vol 406, 24 August 2000, 871-873

Agreement with
Experimental
Observations. Cu.

Channel width of
200nm with a channel
spacing of 1000nm.

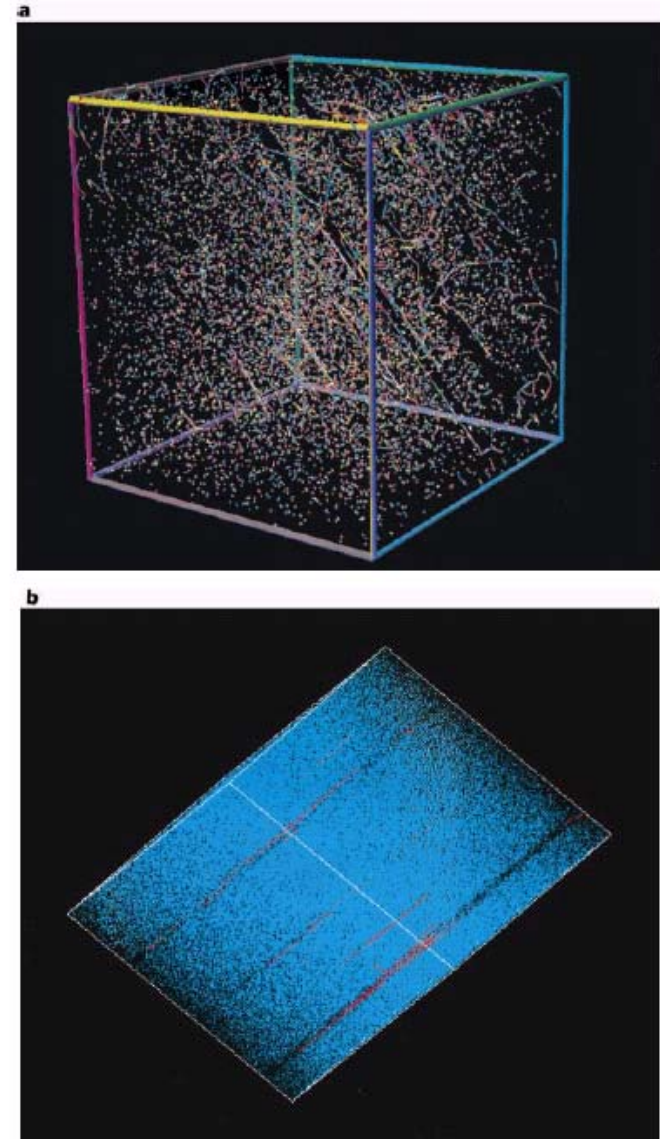
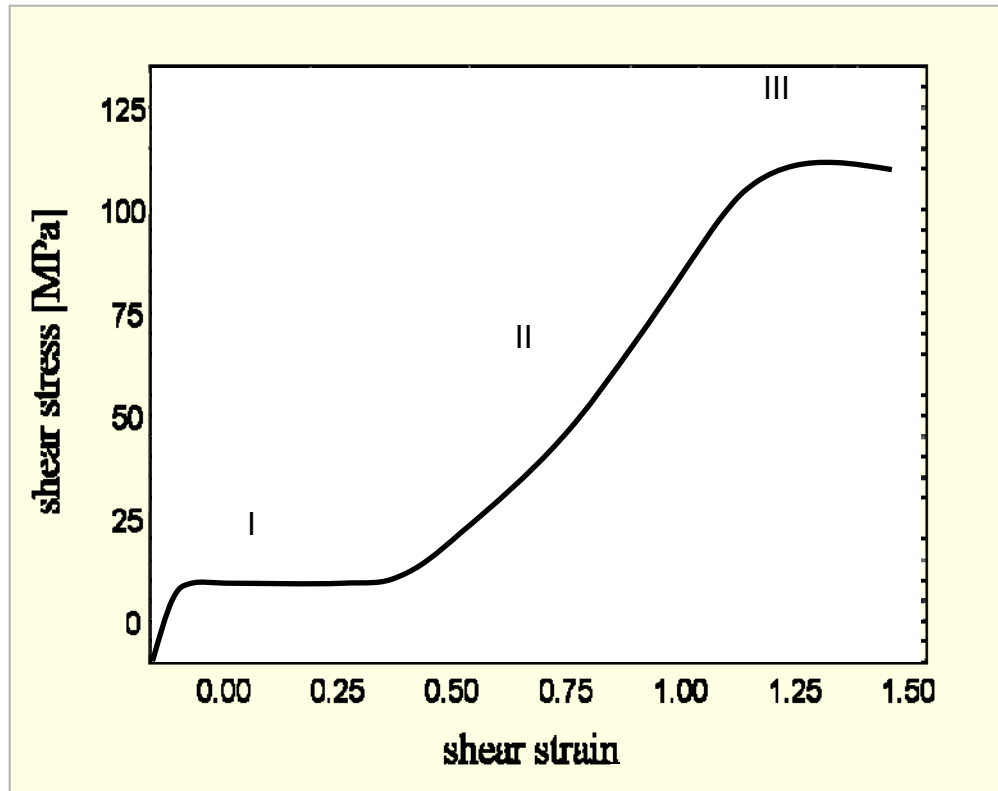


Figure 4 Dislocation dynamics results of channel formation and flow localization. **a**, Results of DD simulation in Cu irradiated to $\rho_B = 8.24 \times 10^{21} \text{ m}^{-3}$ with an initial network dislocation density of $\rho_H = 10^{12} \text{ m}^{-2}$. Shown is the 10- μm side computational cell containing the dislocations and point defects with defect-free channels. **b**, Two-dimensional projection of **a**.

DD methodology must be able to address the elementary processes in fcc crystal plasticity



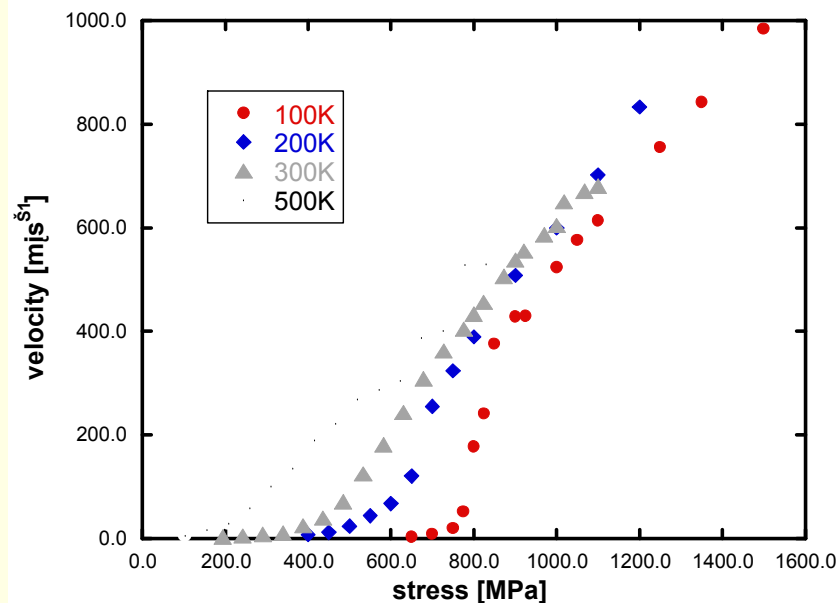
- Stage I: ‘easy’ dislocation glide (primary planes activated)
- Stage II: forest hardening (dislocation reactions \otimes junctions & locks)
- Stage III: recovery (cross-slip)

Single crystal plasticity: uniaxial tensile tests in fcc metals

Further developments towards dislocation mobility laws in bcc

Mobility law in bcc Fe (Mark Gilbert-UKAEA)

- Calculations for pure Fe completed → now doing Fe-Cr



Velocity-stress dependence of a screw dislocation in Fe gliding on a {112} plane

- Simulations in BCC are slower than in FCC → we are exploring other methods
- We have developed a methodology to study the thermodynamics and kinetics of dislocations (P. Schuck & B. Sadigh).
- This could provide the same laws w/o the need for large-scale MD simulations



Free energy of dislocation core atoms (screw & edge)

Carbon sputtering yield as a function of energy

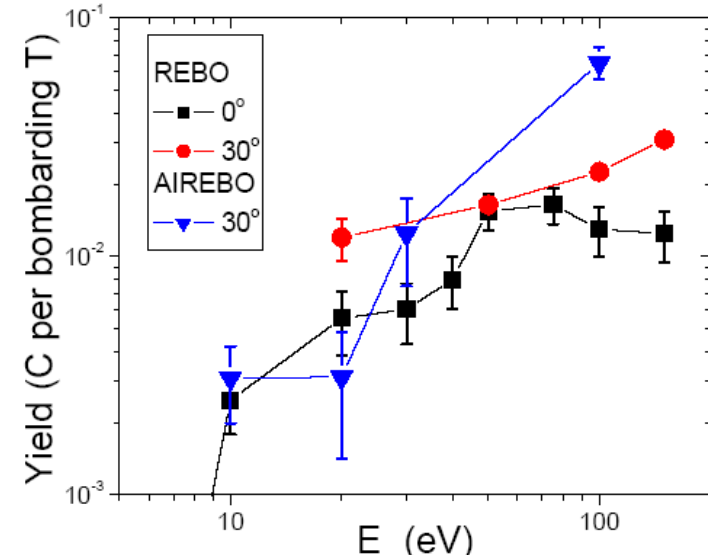
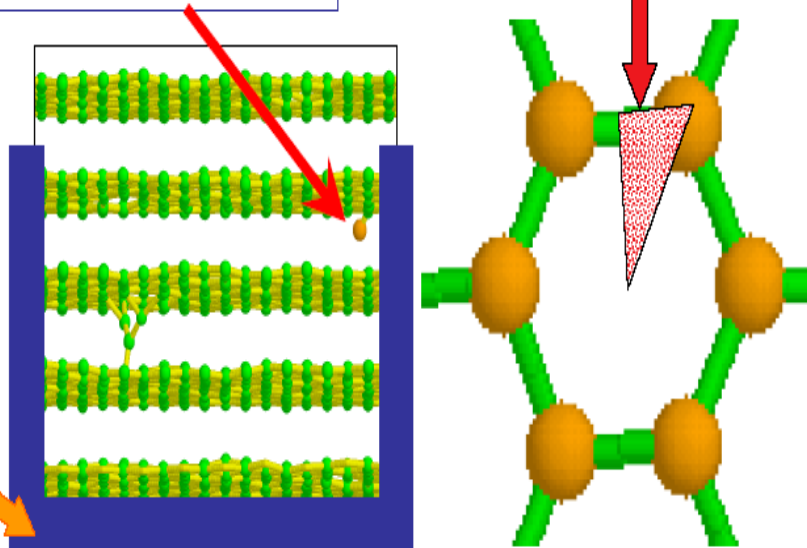
First sputtering calculations using AIREBO

runs with 500-2000 atoms

MDCASK (LLNL): highly parallel, variable time step, Potential: REBO+long range+ZBL
Targets: 500-40,000 C atoms, 300-600 K

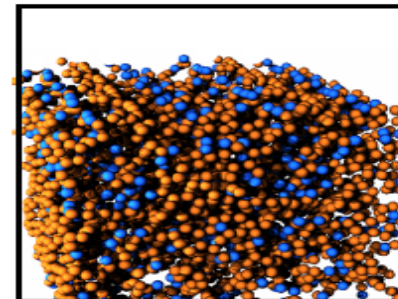
H/D/T projectiles, 5-300 eV, several angles of incidence, hitting an irreducible region on the surface.

Thermostat at sides and bottom to minimize boundary effects



REBO and AIREBO yields are the same within a factor of 2-4.

Runs with bigger/different samples in progress



Irradiation Modes

- Fusion neutrons (what we expect), Fission neutrons (what we have), high energy protons (SPALLATION, what we can have)

Defect / Gas production (in steels)	Fusion neutrons (3-4 GW reactor, first wall)	Fission neutrons(BOR 60 reactor)	High energy protons (590 MeV)
Damage rate [dpa/year]	20-30	~ 20	~ 10
Helium [appm/dpa]	10-15	≤ 1	~ 130
Hydrogen [appm/dpa]	40-50	≤ 10	~ 800

WHAT APPEAR CRITICAL IS THE CONTENT OF IMPURITIES IN THE IRRADIATED SAMPLES

Main Irradiation Conditions

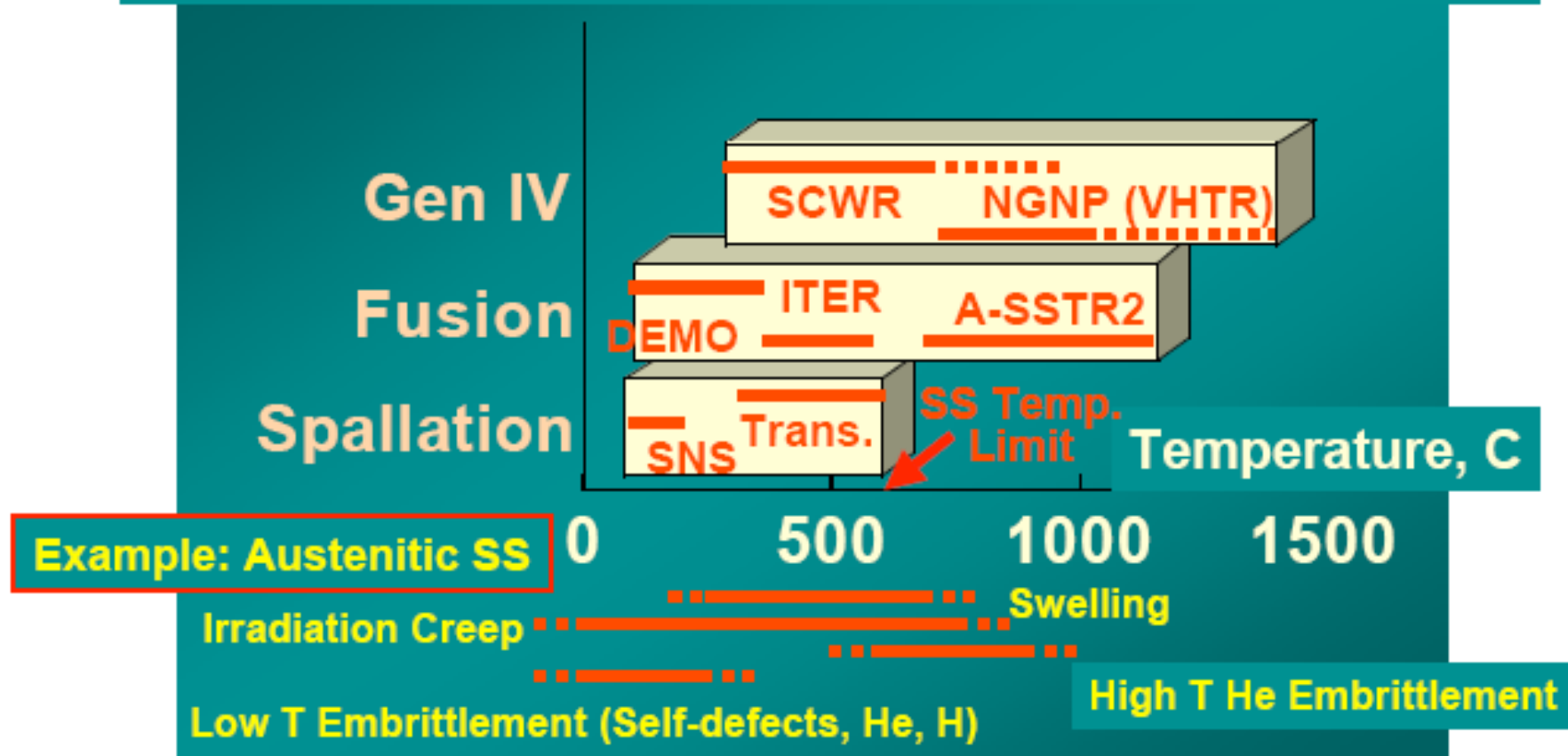
	ITER	DEMO	Reactor
Fusion Power	0.5 GW	2-2.5 GW	3-4 GW
Heat Flux (First Wall)	0.1-0.3 MW/m ²	0.5 MW/m ²	0.5 MW/m ²
Neutron Wall Load (First Wall)	0.78 MW/m ²	< 2 MW/m ²	~2 MW/m ²
Integrated wall load (First Wall)	0.07 MW/m ² (3 yrs inductive operation)	5-8 MW.year/m ²	10-15 MW.year/m ²
Displacement per atom	<3 dpa	50-80 dpa	100-150 dpa
Transmutation product rates (First Wall)	~10 appm He/dpa ~45 appm H/dpa	~10 appm He/dpa ~45 appm H/dpa	

Fission Reactors: 0.2 to 0.3 appmHe/dpa

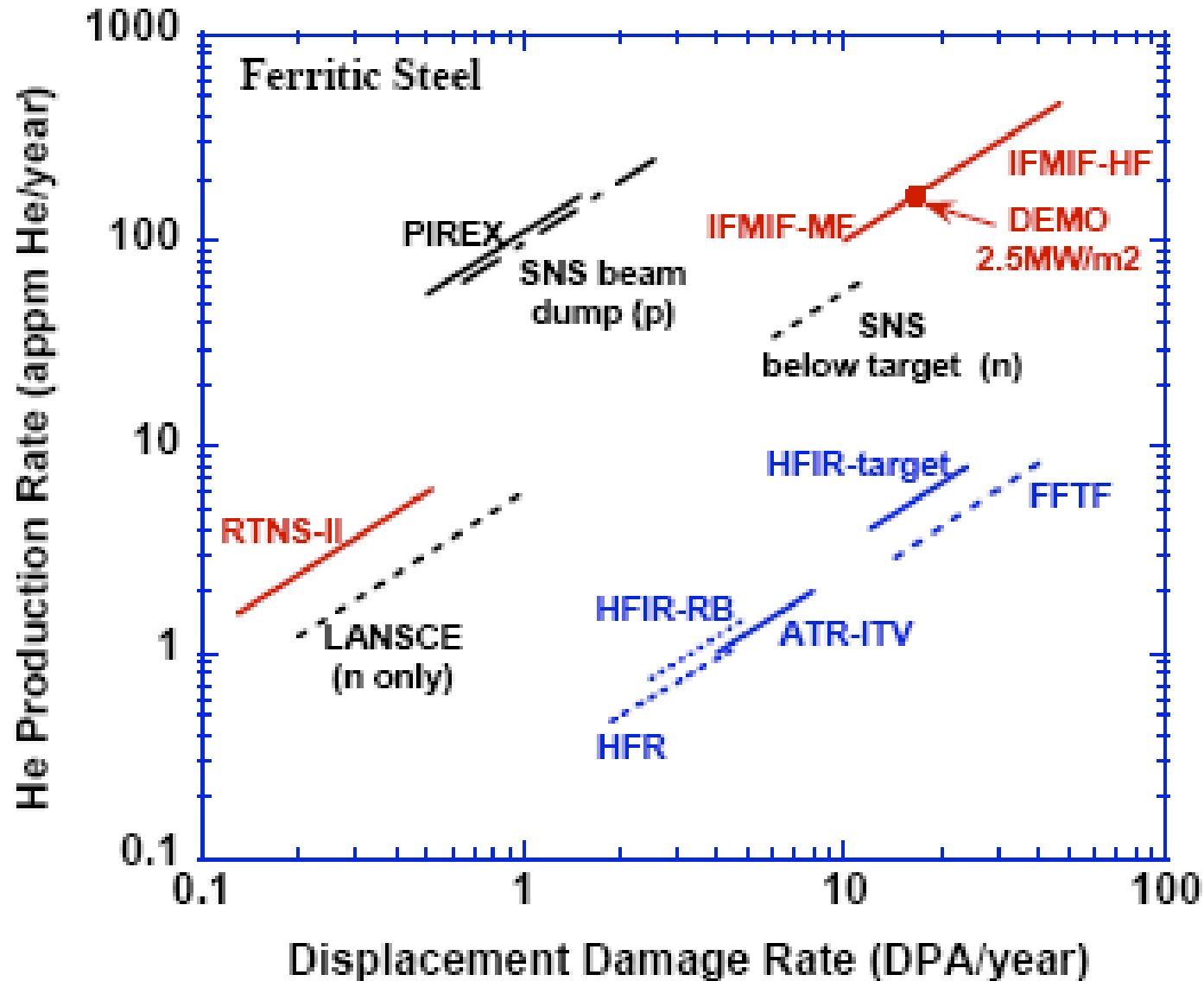


Increasing Challenge

Operating Temperatures and Radiation Effects



Comparison of He and Damage Production Rates for Fission, Fusion-relevant and Spallation Neutron Facilities

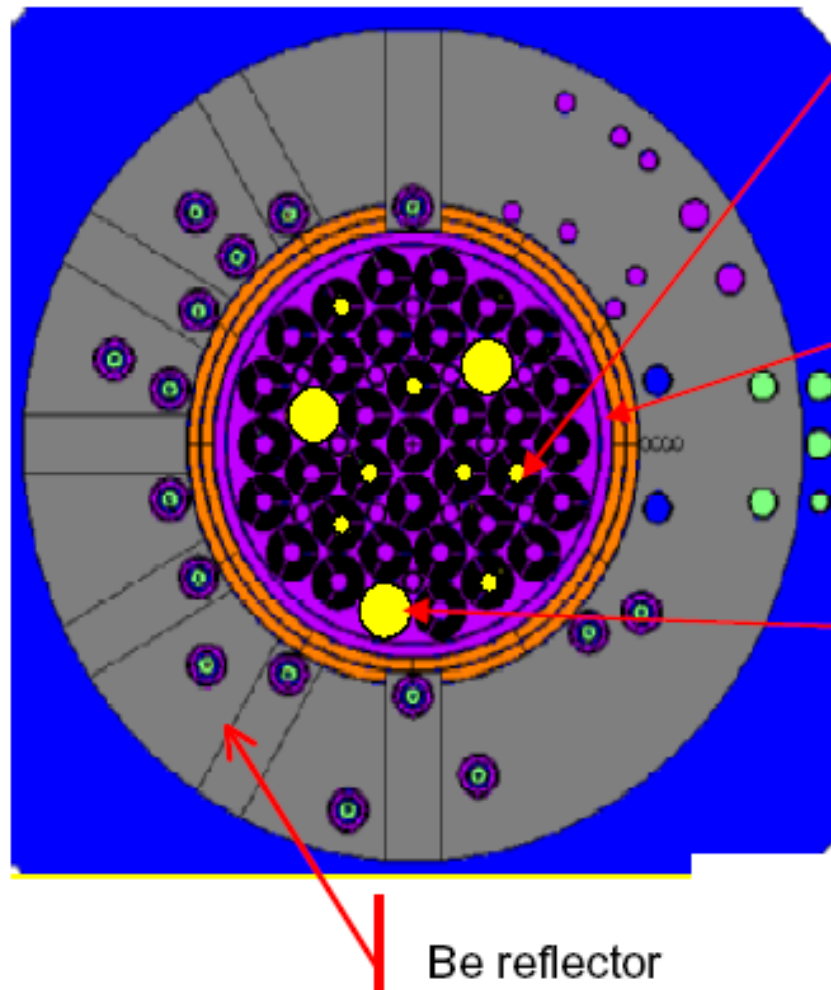


Jules Horowitz Nuclear Fission Experimental Reactor

*In-core material
experiment:*

*Fast flux $\leq 5 \cdot 10^{14}$ n/cm²/s
= 16 dpa/year*

*Ex-core fuel experiment:
Thermal flux $\leq 4 \cdot 10^{14}$
n/cm²/s
= 540 W/cm for 1% U5
Fast flux $\leq 7 \cdot 10^{13}$ n/cm²/s*



**In-core
elementary
location**
(Dia. ~30 mm)

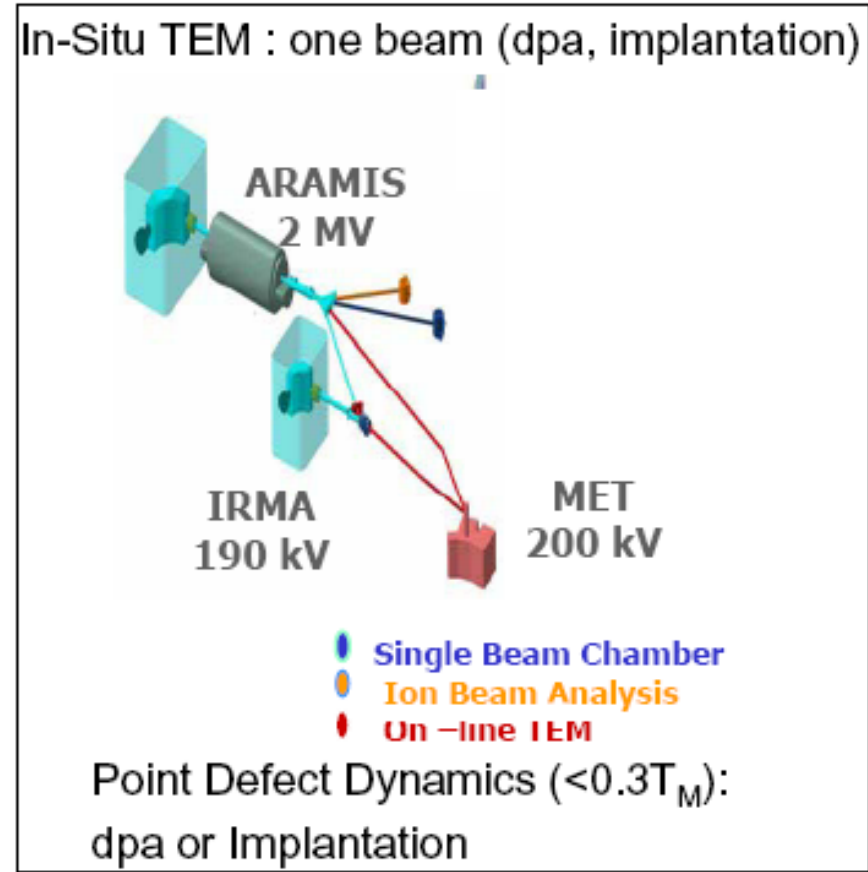
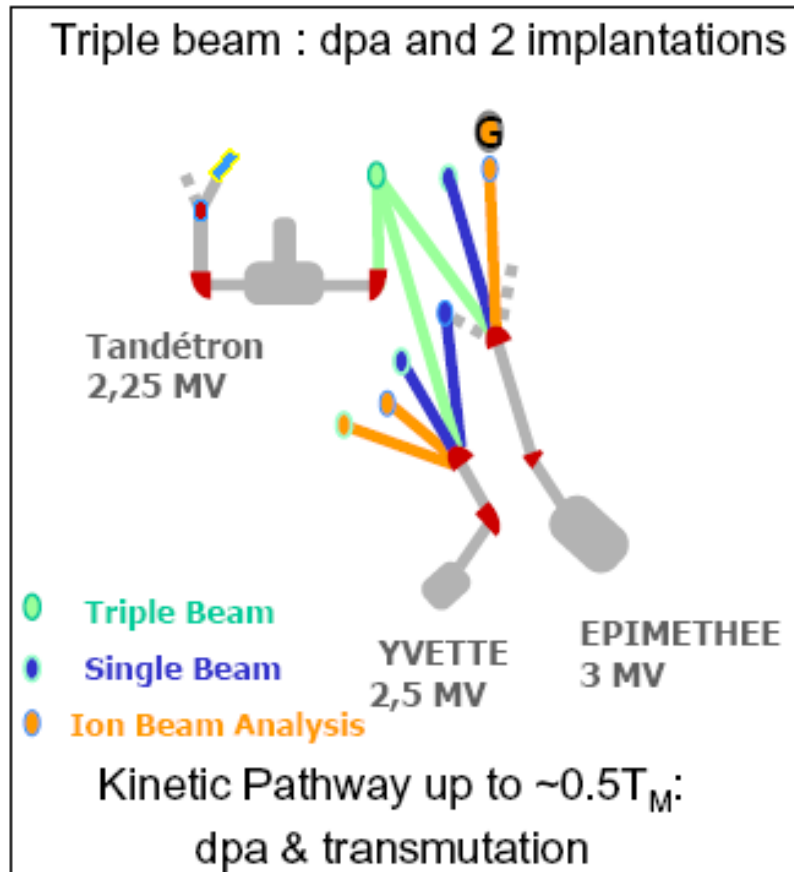
Pressure tank
(Dia. ~683 mm)

**In-core triple
location**
(Dia. ~90 mm)

Be reflector

Joint Accelerators for Nano-Science & Numerical Simulation

Modelling Oriented Experiments with Rapid Feedback



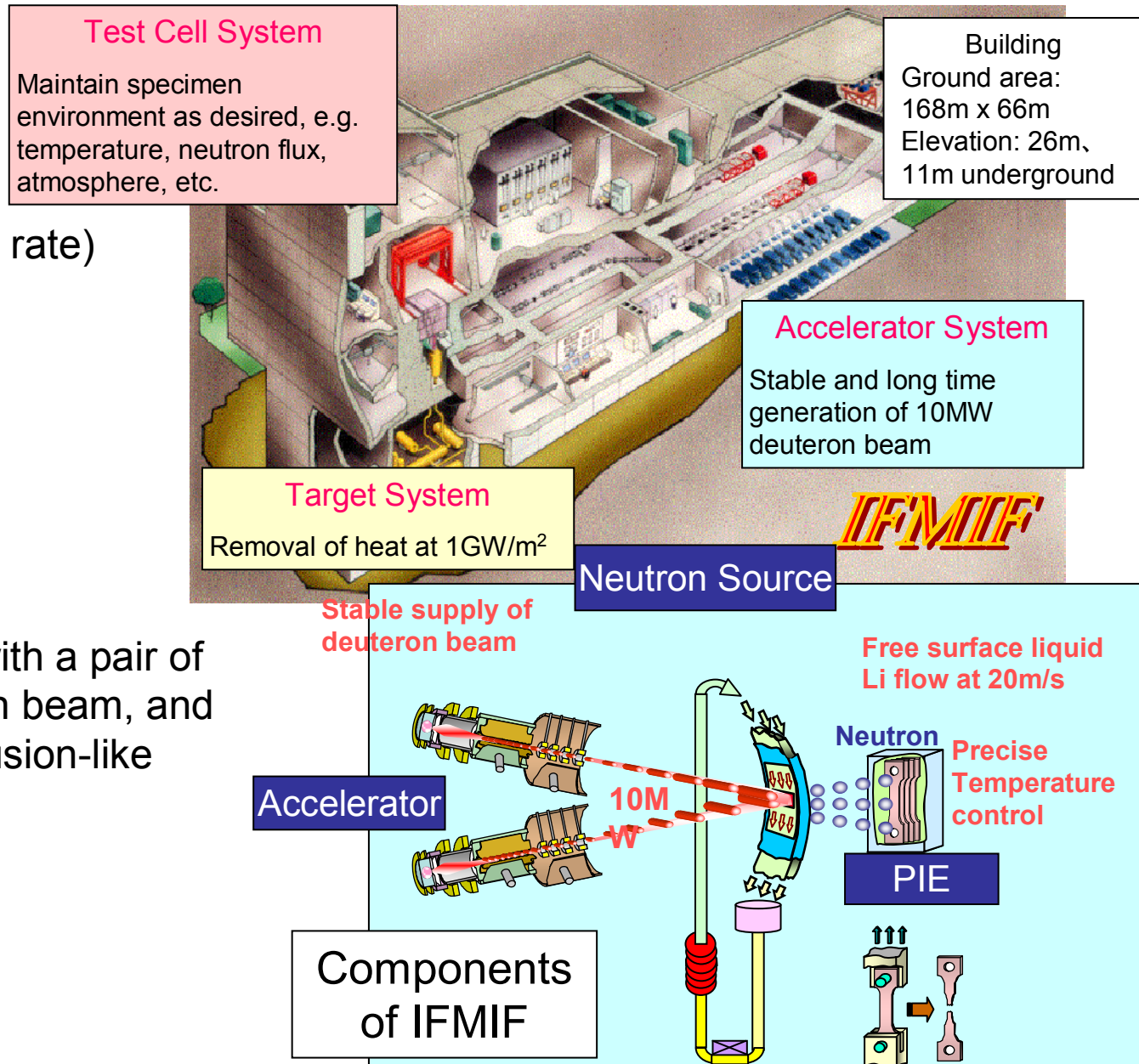
Users' Requirements for IFMIF

Major Requirements

- Irradiation volume (dpa rate)
0.5L (>20 dpa*/year)
6.0L (> 1 dpa/year)
7.5L (>0.1dpa/year)
- Availability: 70%

Type

Hit a liquid Li jet target with a pair of 40MeV, 125mA deuteron beam, and produce neutrons with fusion-like energy spectrum

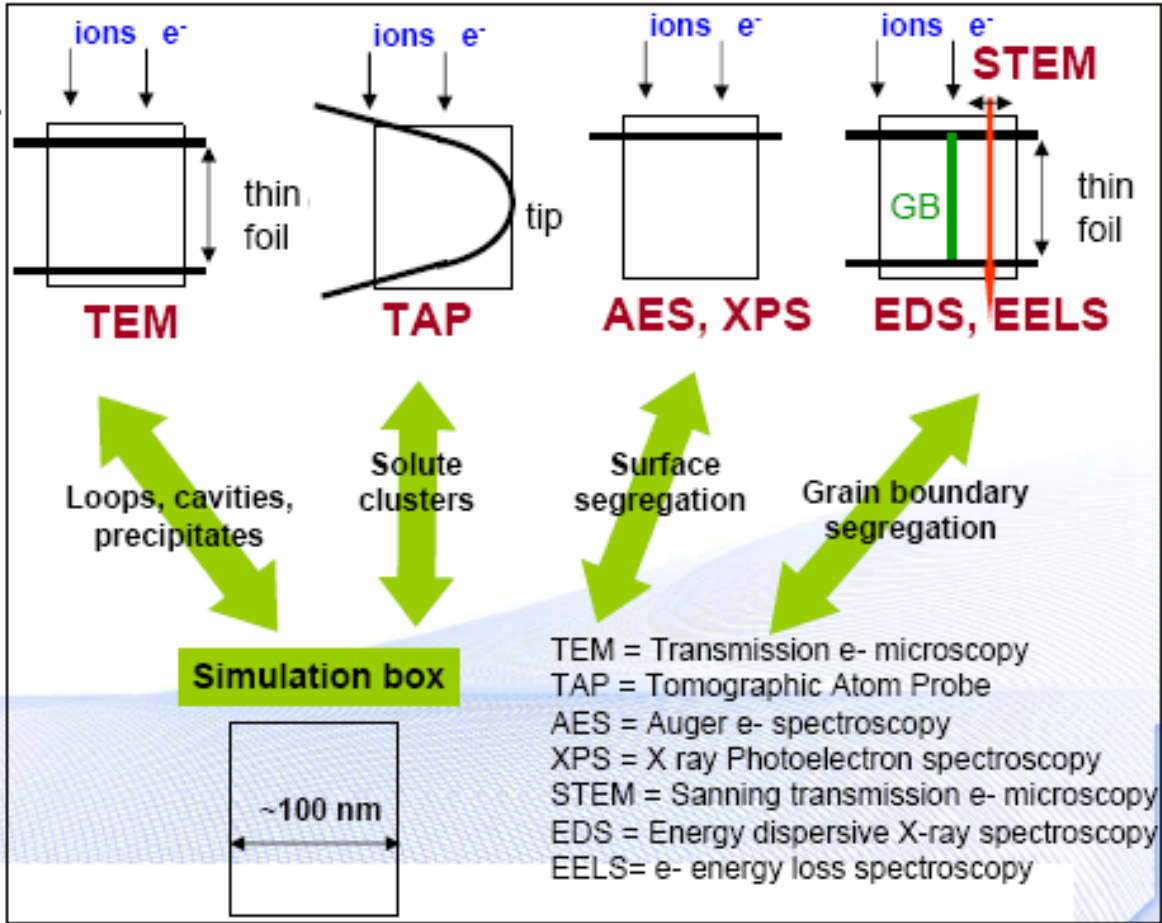
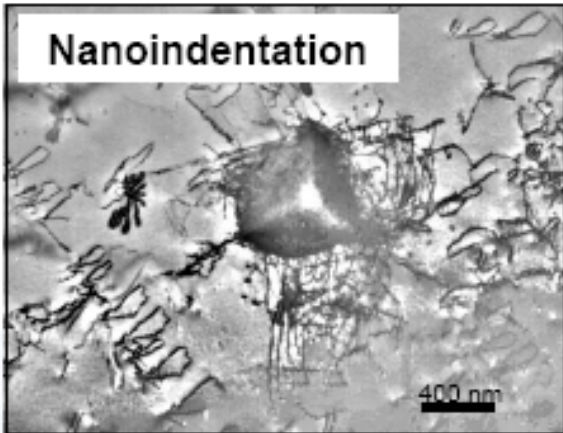


Thanks for your attention

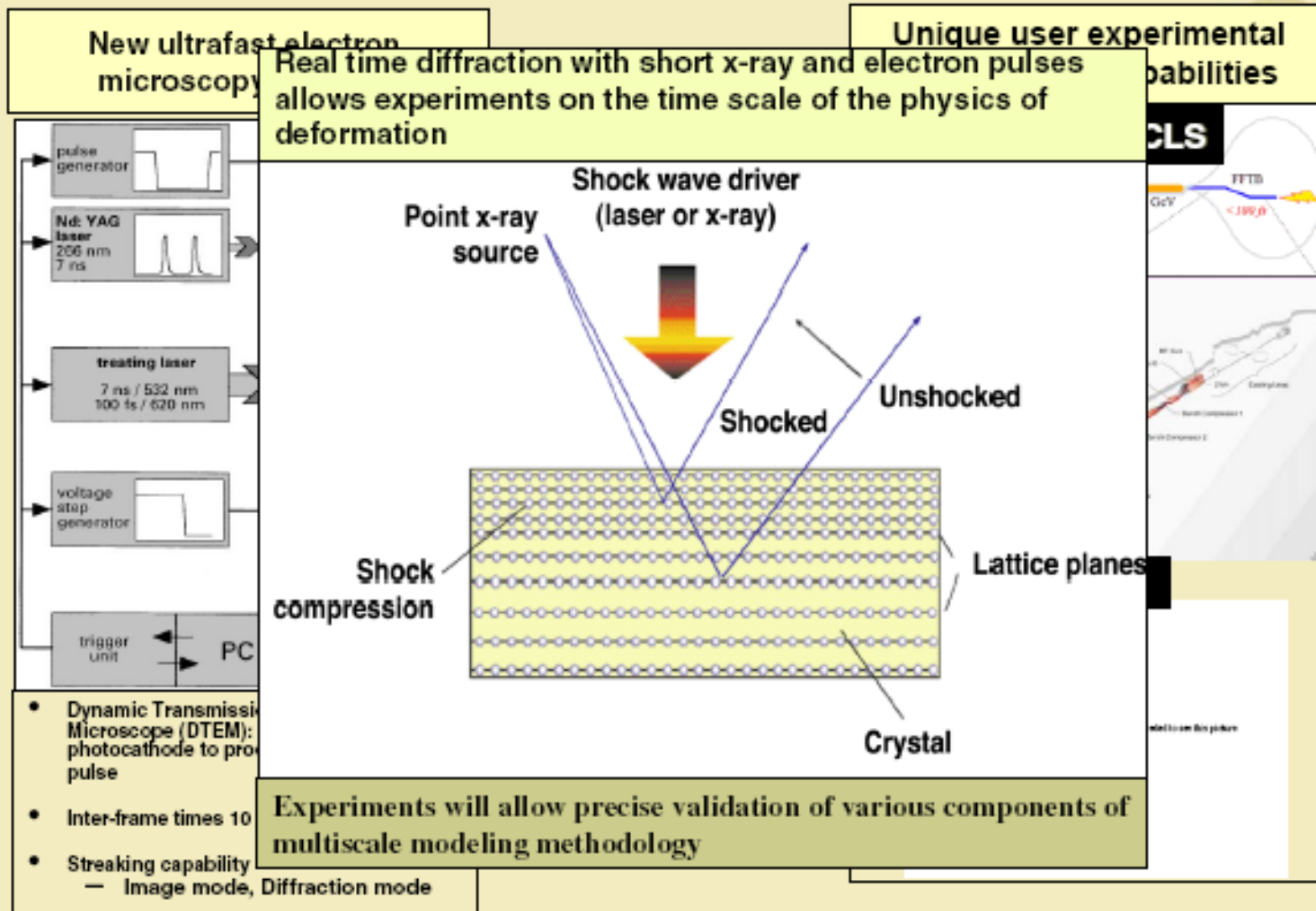
Irradiation → **Charged particles: Dual/Triple Beam + in situ TEM**

Direct observation →

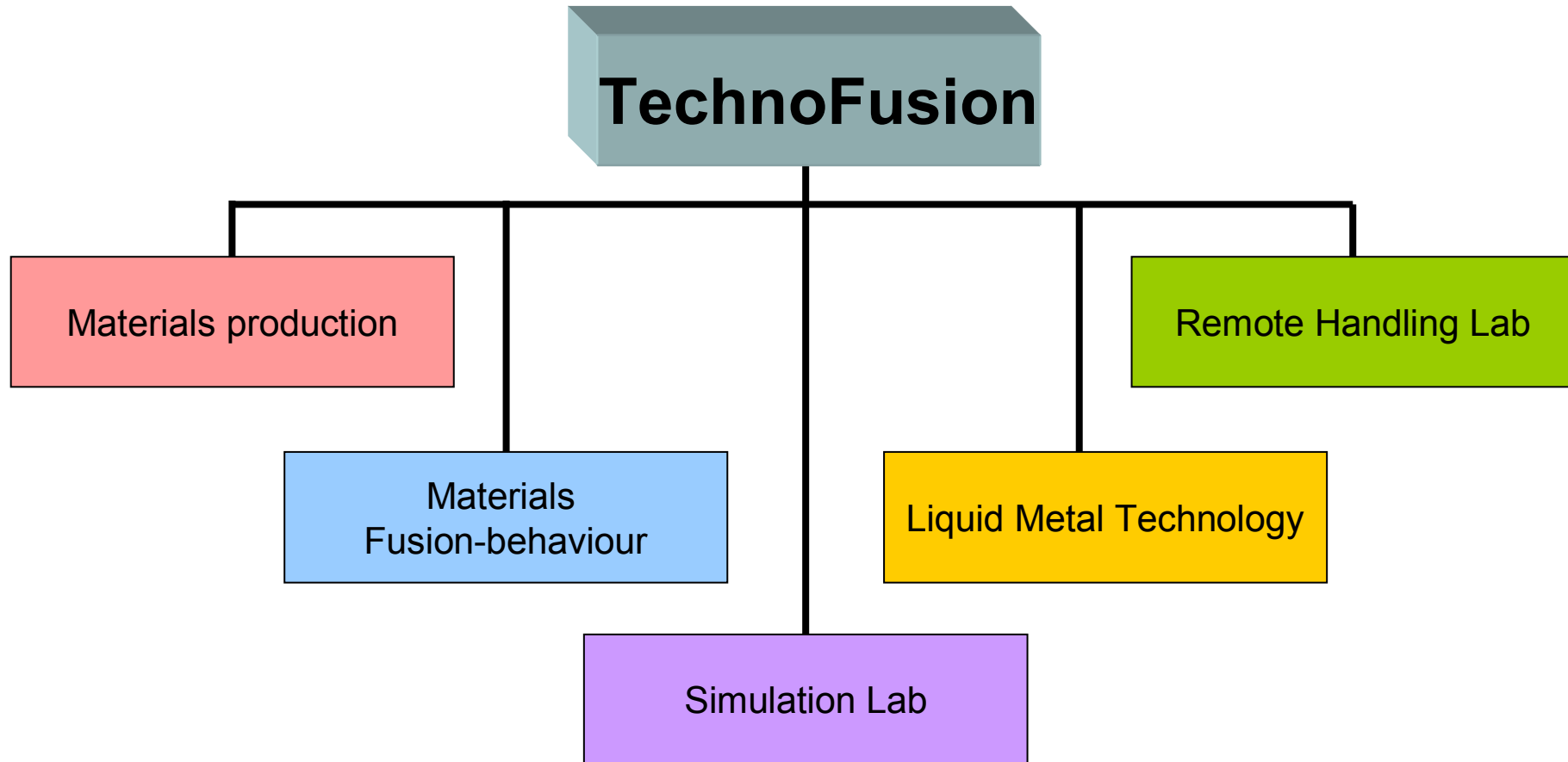
Mechanical testing ↓



Experimental validation is essential - we are developing new ultrafast e- and x-ray diagnostics of materials under extreme conditions

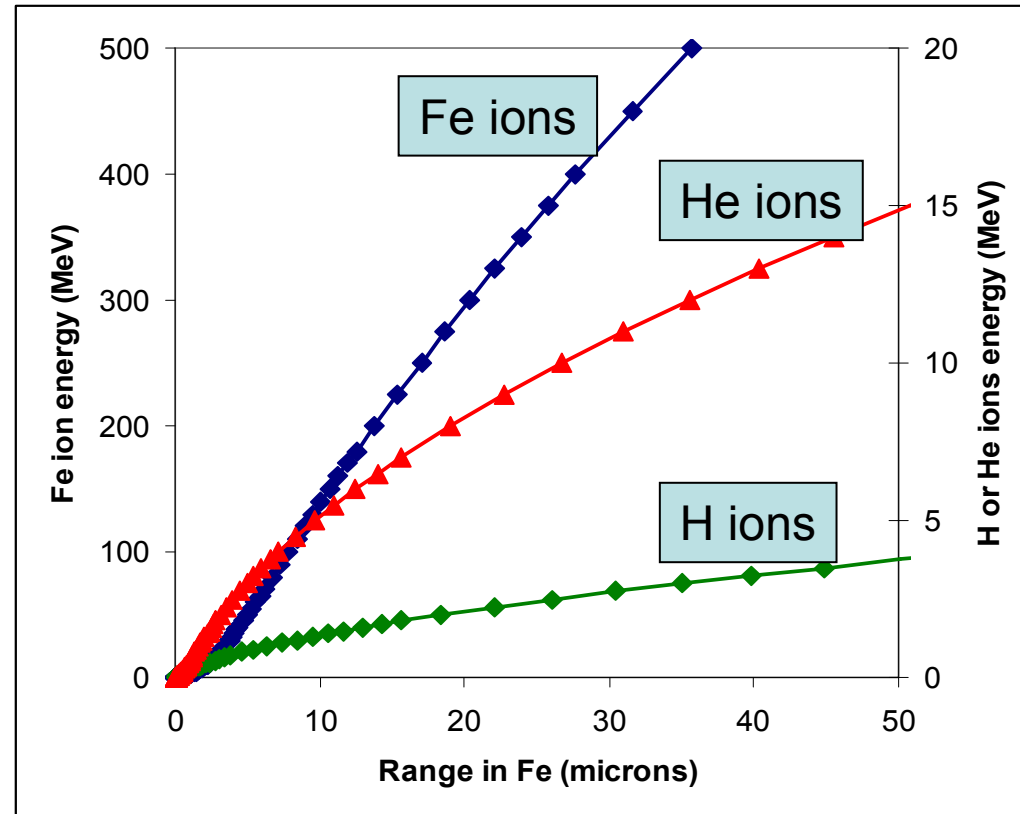


TechnoFusion

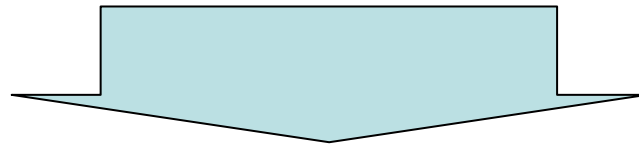


In each area a number of experimental facilities
(some of them unique) are foreseen

The goal is to go up around an order of magnitude beyond the JANNUS implantation range



An irradiated thickness of around 20-25 microns should be accessible



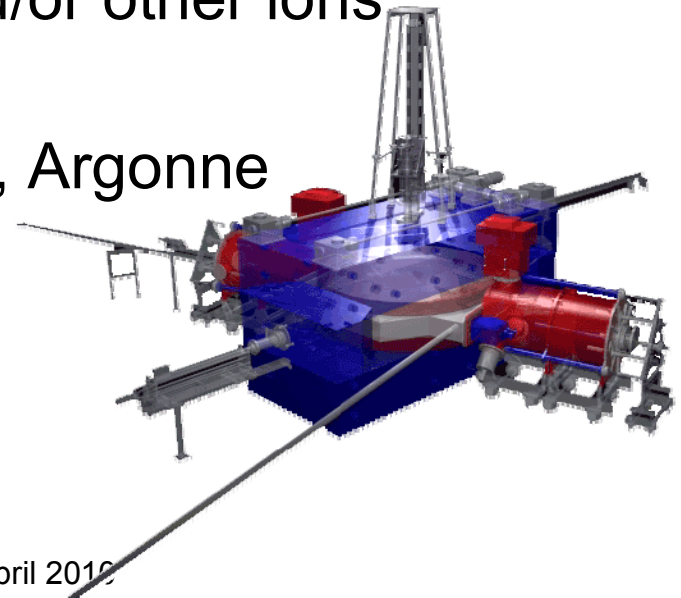
At least a few grains for most of the materials of interest

Accelerators

- A set of three accelerators to simulate neutron irradiation damage:
- a **cyclotron for heavy ions** (Fe, W, Si, C, others).
Energy range: a few hundred MeV; or a

Proton Accelerator 40-60 MeV

- A tandem electrostatic accelerator for He (and/or other ions). Energy range: around 10 MeV
- An electrostatic accelerator for H (and/or other ions).
Energy range: a few MeV
- Reference facilities: JANNUS, TIARA, Argonne



Proposal of a PWI facility for Reactor Materials

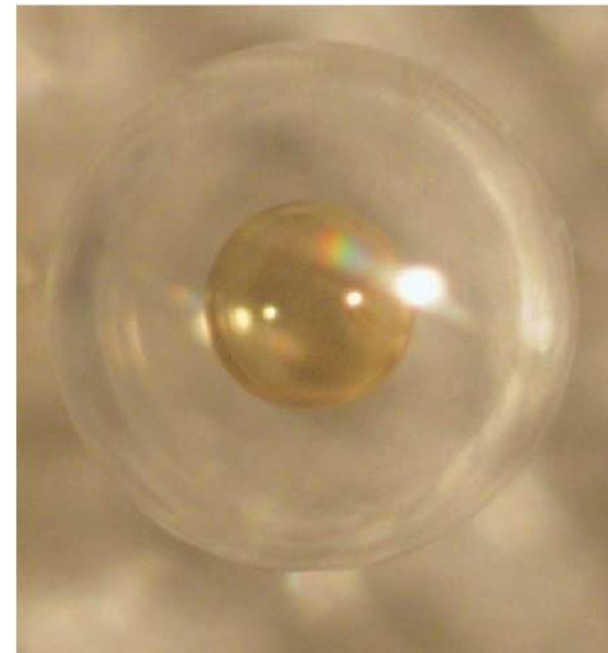
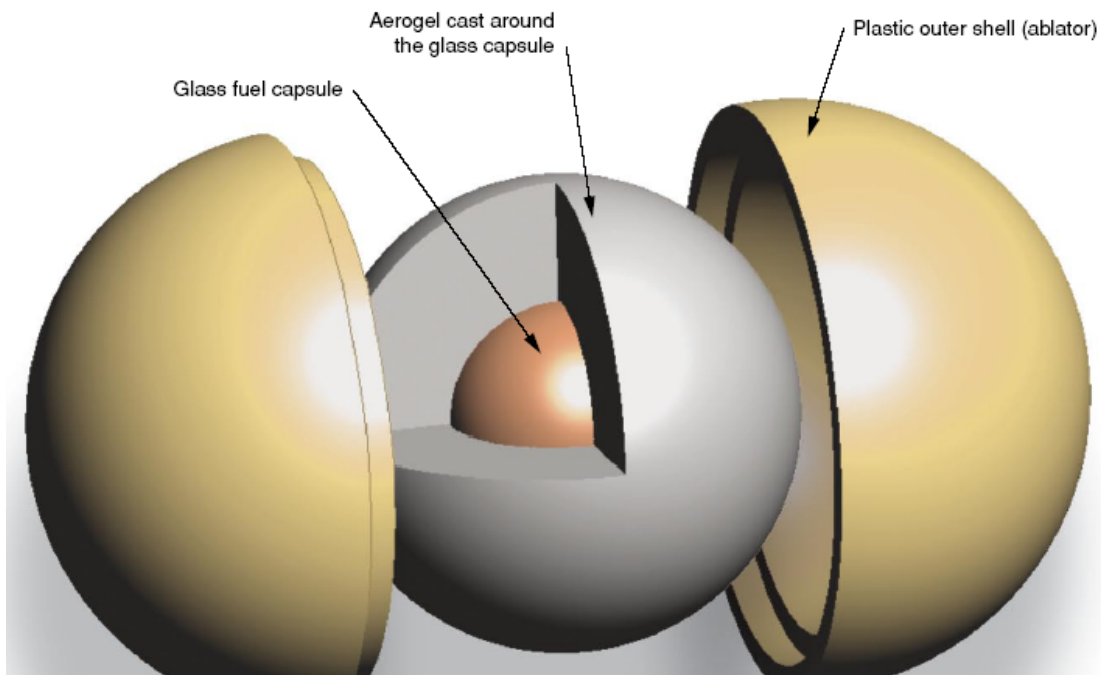
Goal: To simulate the condition expected for the interaction of the plasma with solid elements under reactor-type fusion devices

Background:

- Particle fluxes at the divertor in ITER and in reactors $> 10^{24}$ ions/m².s
- Transient thermal loads (ELMS and disruptions) \sim MJ/m²
- Temperature between transients: few 100°C (not loaded areas) to 1500°C (loaded areas)
- Frequency and duration of transients : few Hz to one every several pulses , 0.1-10 ms
- ITER FW materials: CFC, W, Be
- DEMO FW materials: W,

What we request from Structural Materials ??

- **Work at High Temperatures**
- **Resistance to
High levels of neutron irradiation**
- **Resistance to
High mechanical stresses**
- **Resistance to
High thermo-mechanical stresses**



Target Fabrication: key aspect in materials development for Inertial Fusion (double layer/ LLNL) and Fast Ignition (ILE/Norimatsu)

INTRODUCTION: Assessment from Laplace 1820

*An intelligent being who, at a given moment, knows all the **forces** that cause nature to move and the **positions** of the objects that it is made from, if also it is powerful enough to analyze this data, would have described in the same formula the movements of the largest bodies of the universe and those of the lightest atoms. Although scientific research steadily approaches the abilities of this intelligent being, complete prediction will always remain infinitely far away.*

INTRODUCTION: Assessment from Dirac 1929

*The general theory of **quantum mechanics** is now almost complete. The underlying physical laws necessary for the mathematical theory of a large part of physics and the whole of chemistry are thus completely known, and the difficulty is only that the exact application of these laws leads to equations much too complicated to be soluble.*

Model	Type	Scaling	N_{\max}^1
Full solution of Schrödinger equation	quantum mechanical, ab initio	$O(e^N)$	1
HF (Hartee-Fock)	quantum mechanical, ab initio	$O(N^{4-8})/$ $O(N)$	50
DFT (density functional theory)	quantum mechanical	$O(N^3)/$ $O(N)$	200
TB (Tight-binding)	quantum mechanical (often semiempirical)	$O(N^3)/$ $O(N)$	1000 10000
Many-body potential	classical, semiempirical	$O(N)$	10^7
Pair potential	classical, semiempirical	$O(N)$	10^7

¹This is a very rough estimate of how many atoms N can be simulated in a reasonable time, i.e. a week or so, on a single-processor machine. For multi-electron atoms solution of the full Schrödinger equations is very hard even for a single atom.

First principles information:
atomic numbers, crystal structure (lattice, atomic positions)

Choose initial electronic density $\rho(\mathbf{r})$

Calculate effective potential using the LDA Equation 1

$$V_{\text{eff}}(\mathbf{r}) = V_{\text{ion}}(\mathbf{r}) + \int d^3\mathbf{r}' V_{ee}(\mathbf{r} - \mathbf{r}')\rho(\mathbf{r}') + \frac{\delta E_{\text{xc}}[\rho]}{\delta\rho(\mathbf{r})}$$

Solve Kohn-Sham equations Equation 2

$$\left[-\frac{\hbar^2}{2m} \nabla^2 + V_{\text{eff}}(\mathbf{r}) - \varepsilon_i \right] \varphi_i(\mathbf{r}) = 0$$

Calculate electronic density Equation 3

$$\rho(\mathbf{r}) = \sum_i^N |\varphi_i(\mathbf{r})|^2$$

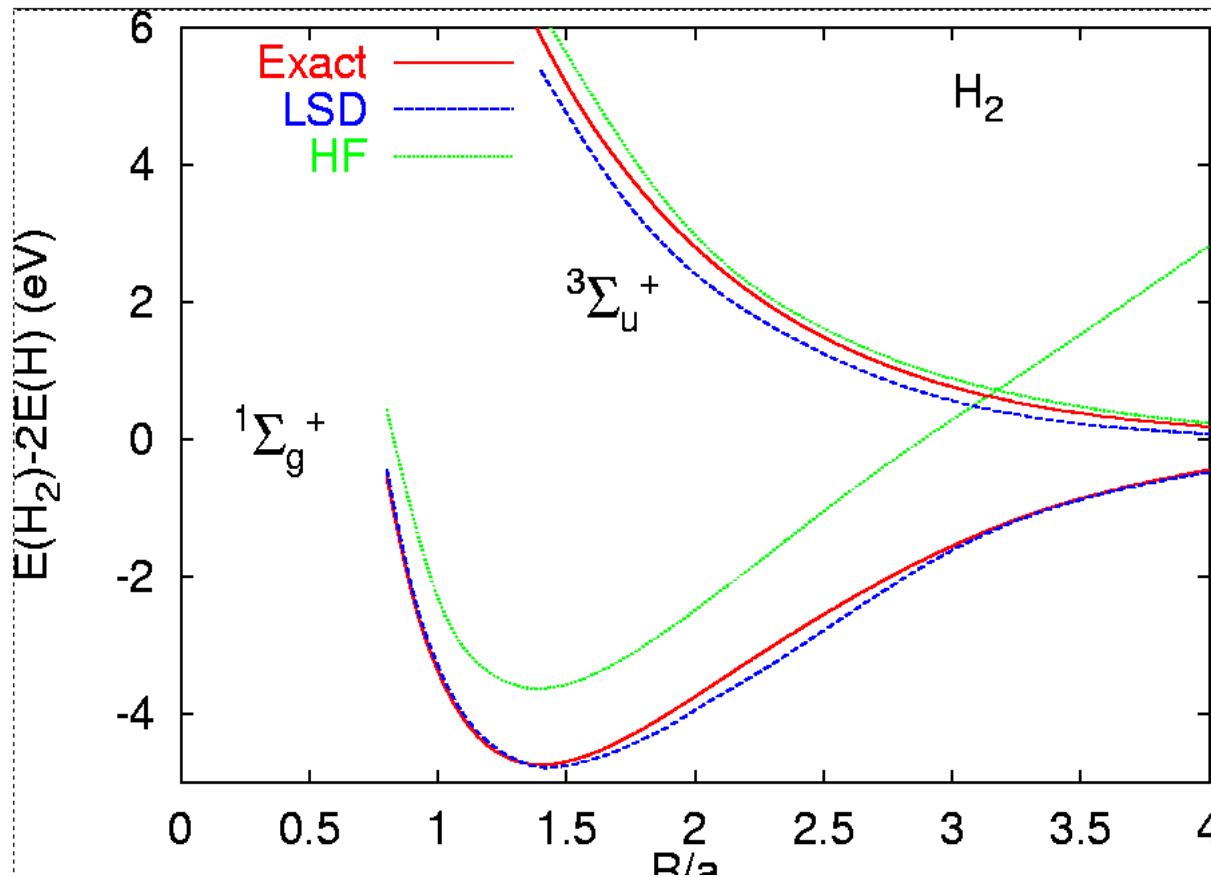
Iterate to self-consistency

Calculate band structure $\varepsilon_i(\mathbf{k})$ In Eq. 2 partial and total DOS, self-consistent Hamiltonian \Rightarrow LDA+DMFT, total energy $E[\rho]$...

Examples of Results

- Hydrogen molecules - using the LSDA

(from O. Gunnarsson)



Beyond BCA Models in collision cascades ⇒ **Molecular Dynamics**

- *Fundamental assumption of BCA*: defects produced in isolation, without interference with nearby recoils.
- Creation of Frenkel pair agitate the lattice over extended distances.
- Thermal spikes models neglects the atomic displacement process.
- ⇒ no simultaneous simulation possible
- **NO POSSIBLE TO DESCRIBE COMPLETELY THE DYNAMICS OF COLLISION CASCADES**
for example the description of cascade interior melting.

MOLECULAR DYNAMICS

- Boundary Conditions (**Periodic**, *Fixed*)
- Constant Volume or Pressure (*Parrinello & Rahman*)
- At the boundary:

Damping of thermal modes *Friction force* (β parameter)
eliminate the excess of energy, *and*

Random Force that simulates the heat of the particle at
the temperature required in the bath, $\vec{R}_i(t)$

Then the particles if this control is used must obey a
Langevin type equation of motion

$$m \frac{d\vec{v}_i}{dt} = \vec{F} + \vec{R}_i(t) - \beta\vec{v}_i$$

MOLECULAR DYNAMICS

Embedded Atom Model (EAM)

- Metal as positively charged ions “*embedded*” in a local electron density.
- Energy of the system from an *embedding* energy and the ion core repulsion.
- Assumption from ***density functional theory***.....

Total electronic energy is a unique function of the local electron density in which the ion is embedded

Local density as superposition of atomic densities of surrounding atoms

$$E_{tot} = \sum_j F(\rho_i) + \frac{1}{2} \sum_{i,j(\neq i)} \Phi(R_{i,j})$$

MOLECULAR DYNAMICS

Stillinger - Weber potential

- Proposed to reproduce the liquid state of Si (also Ge)
from general potential energy function

$$\phi = \sum_i v_1(i) + \sum_{\substack{i,j \\ i < j}} v_2(i, j) + \sum_{\substack{i,j,k \\ i < j < k}} v_3(i, j, k) + \theta(4)$$

only pair and triplet terms considering the strong and directional bonds

$$v_2(r_{ij}) = \varepsilon f_2(r_{ij} / \sigma)$$

$$v_3(\vec{r}_i, \vec{r}_j, \vec{r}_k) = \varepsilon f_3\left(\frac{\vec{r}_i}{\sigma}, \frac{\vec{r}_j}{\sigma}, \frac{\vec{r}_k}{\sigma}\right)$$

ε energy unit and σ length unit

Molecular Dynamics in Zr. Cascade formation and relaxation

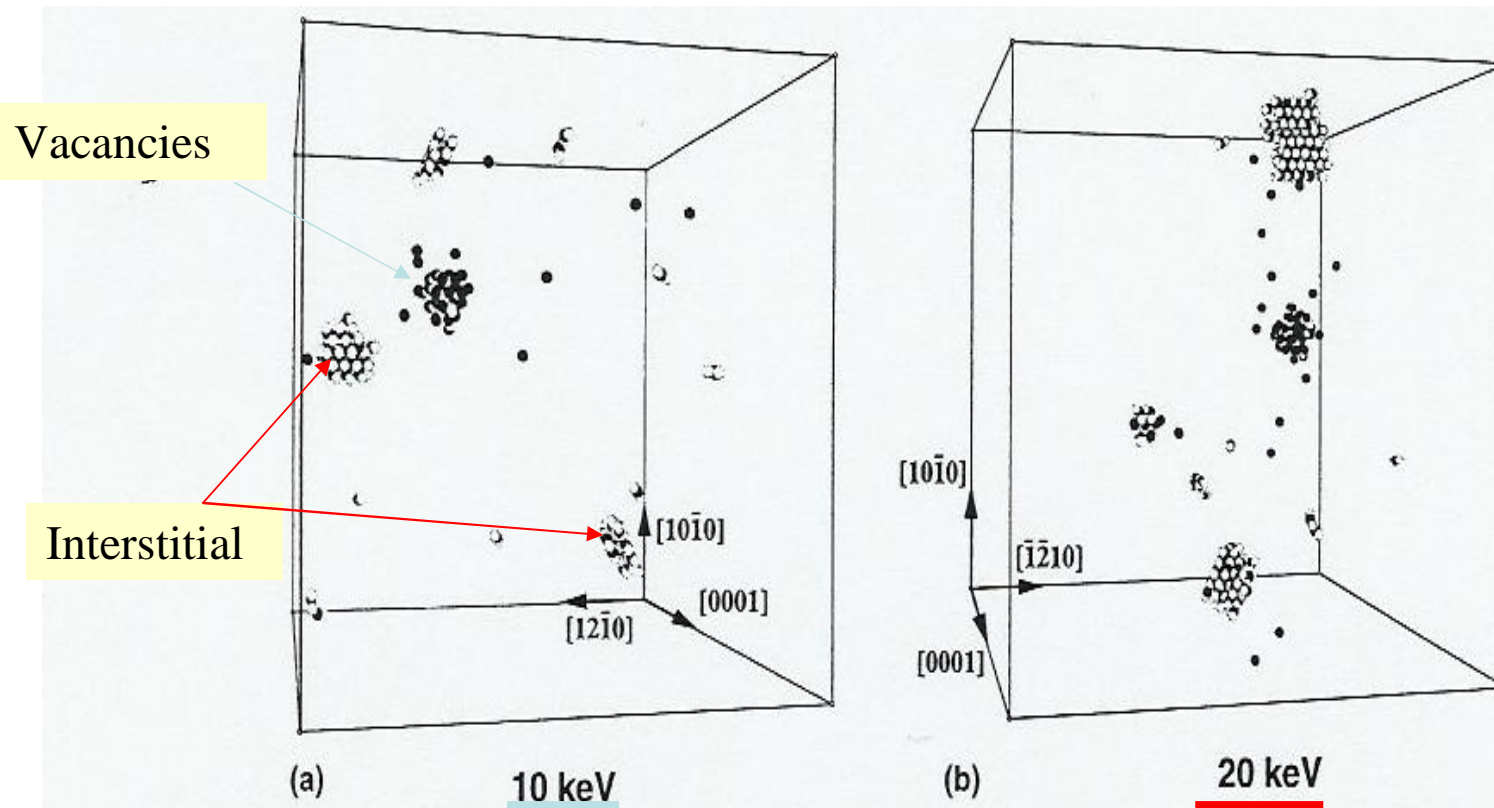


Fig. 3. Computer plots showing the final state of damage of; (a) a 10 keV cascade, and (b) a 20 keV cascade at 600 K, where white spheres represent interstitials and dark spheres indicate vacancies.

F. Gao, D.J. Bacon, L.M. Howe, C.B. So, *Journal of Nuclear Materials* **294** (2001) 288-298

A clear example of Multiscale Modeling in Radiation Damage using the different tools:

Multiscale Modelling of plastic flow localization in irradiated materials. T.Díaz de la Rubia et al., Nature Vol 406, 24 August 2000, 871-873

Vacancy SFT are predominant defects in materials such as Cu, and self-interstitial atom Frank sessile loops in such as Pd.

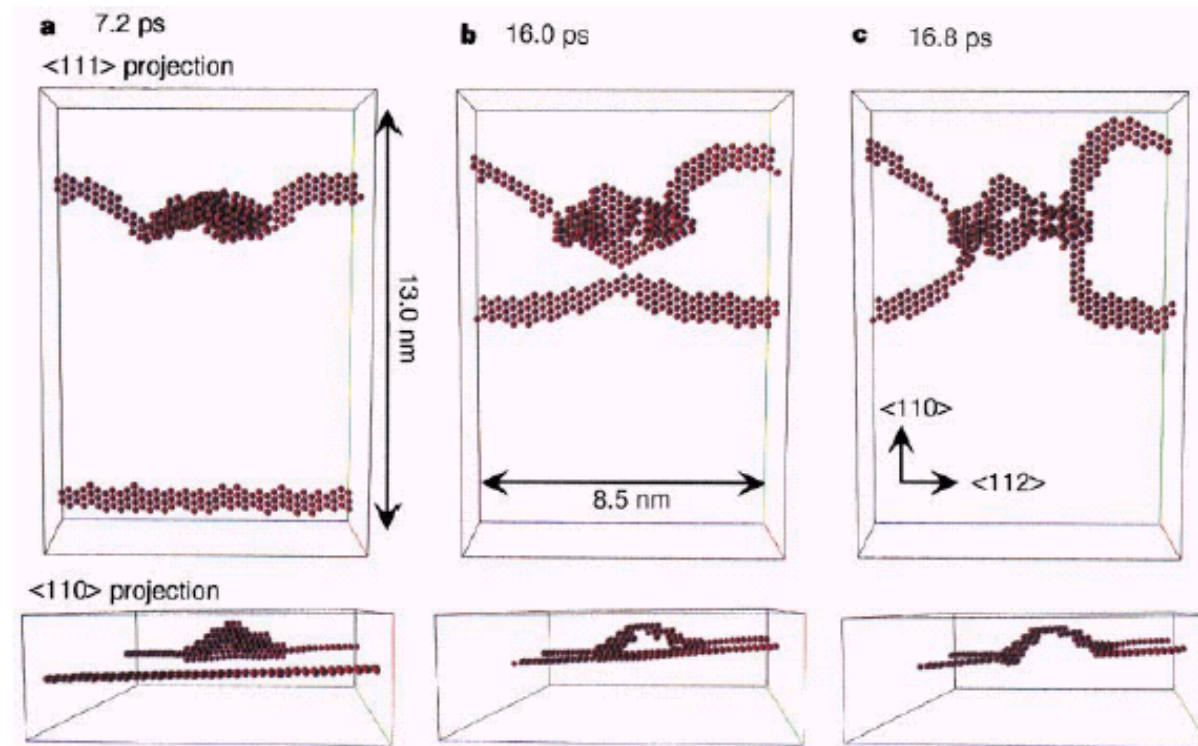
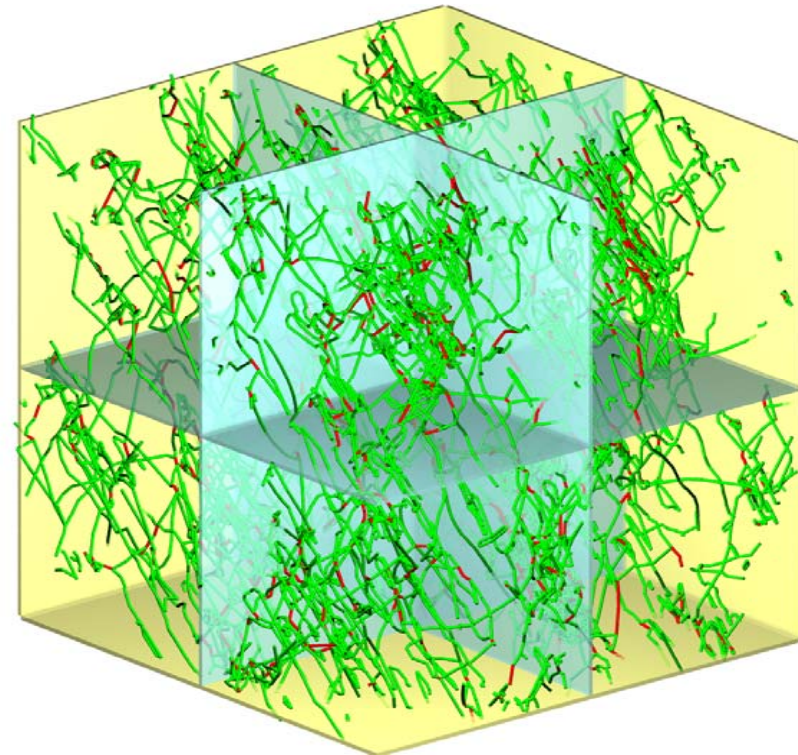
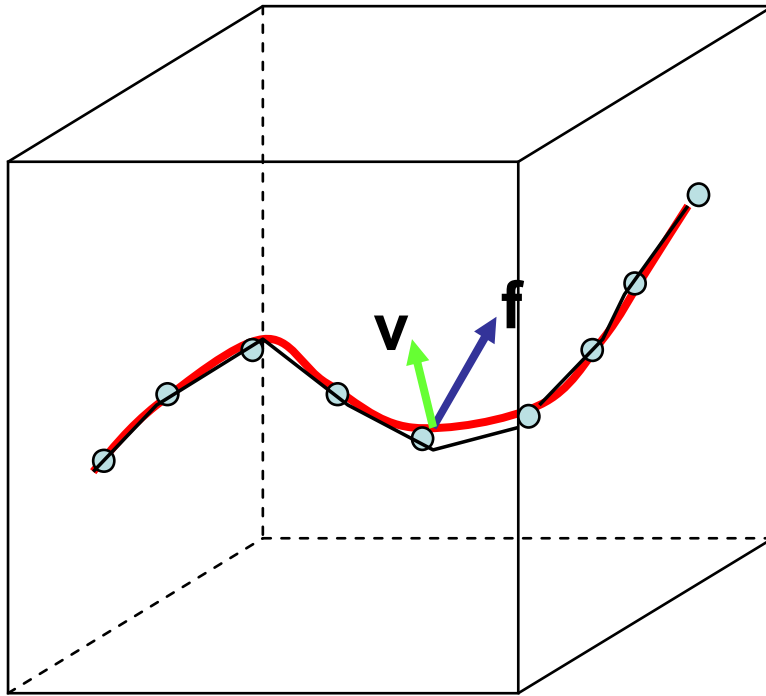
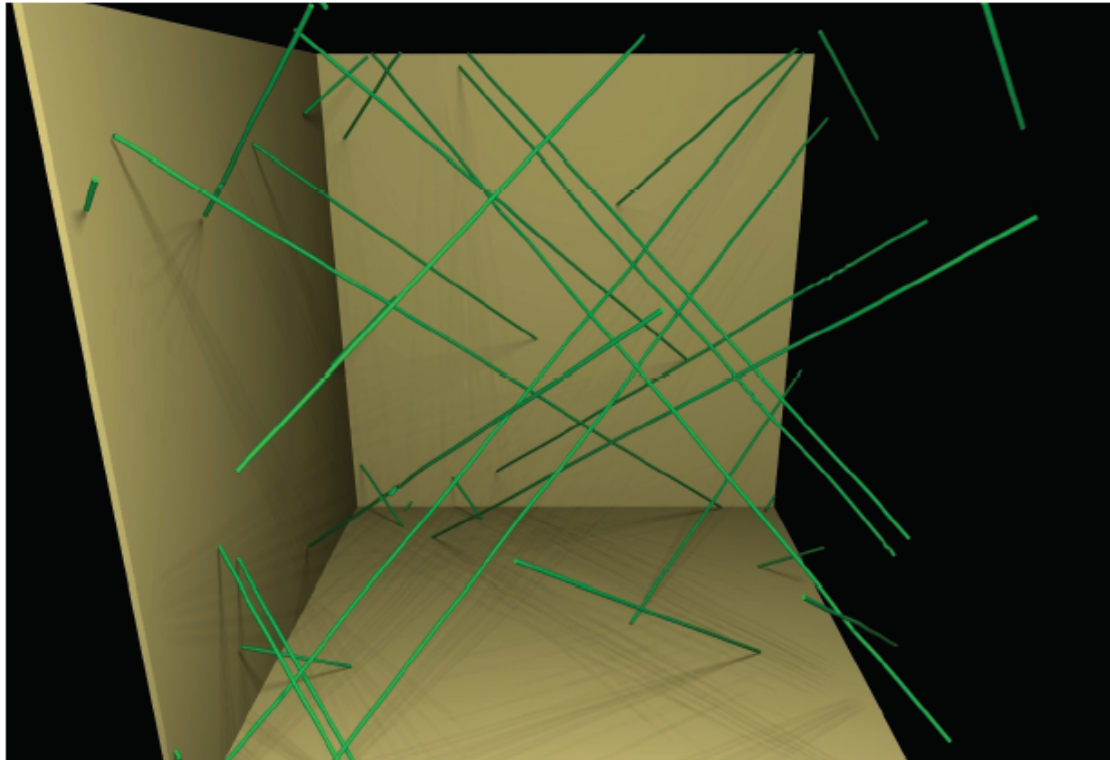


Figure 2 Molecular dynamics simulation of the interaction between an edge dislocation and an overlapping, truncated vacancy stacking-fault tetrahedron (SFT) in Cu. **a–c**, $\langle 111 \rangle$ (top) and $\langle 110 \rangle$ (bottom) projections of high-energy atoms show the motion of two Shockley partial dislocations on their $\{111\}$ glide plane and their interaction with an overlapping vacancy SFT at **a** 7.2, **b** 16.0 and **c** 16.8 ps after application of a 300-MPa

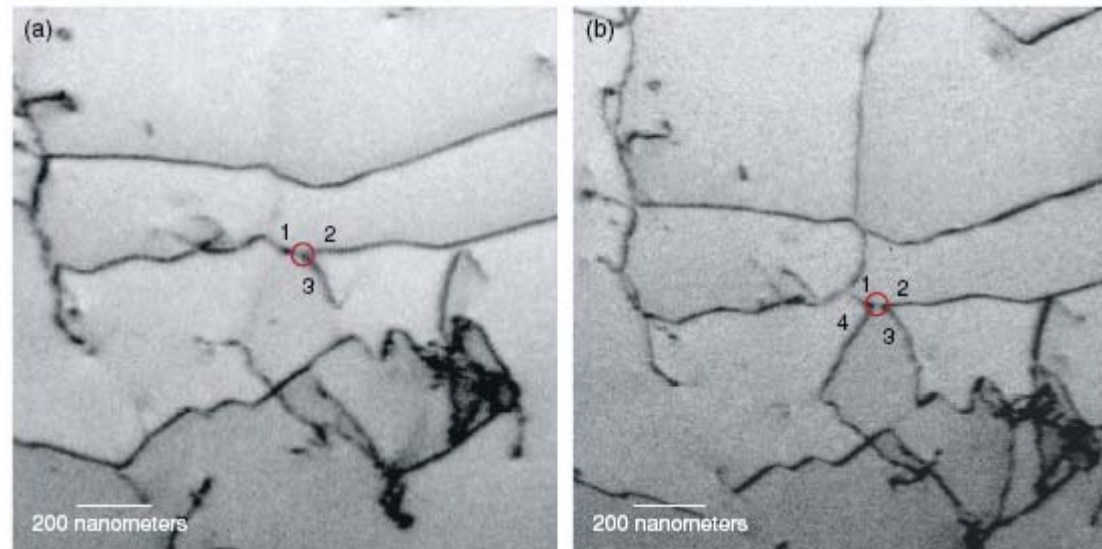
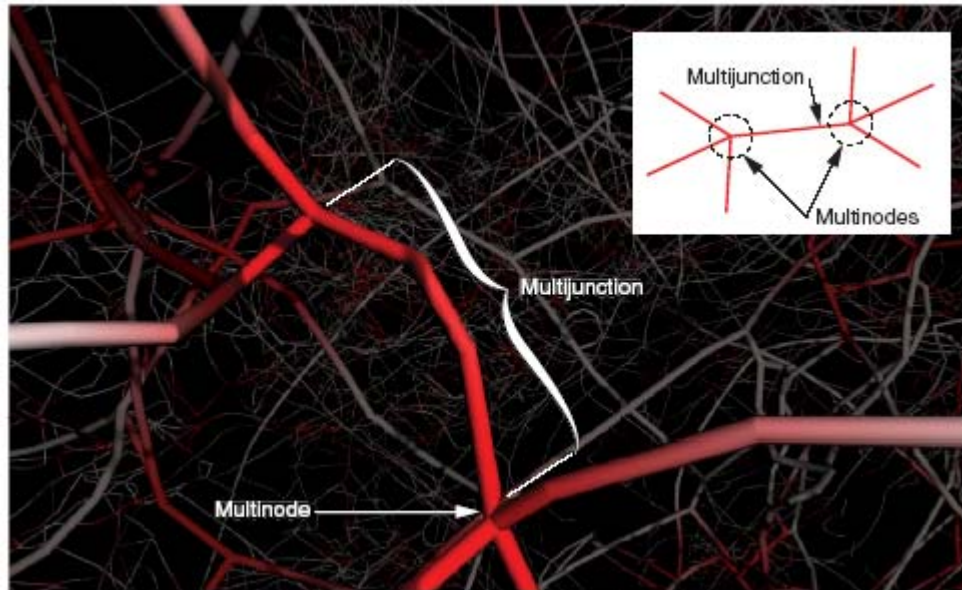
shear stress. A triangular vacancy platelet that is bounded by $\langle 110 \rangle$ directions forms a single SFT. A triangular vacancy platelet bounded by two $\langle 110 \rangle$ and one $\langle 112 \rangle$ directions forms two partial SFTs, one above and one below the initial plane; we define this as an overlapping truncated SFT.



Caja de Simulación en PARADIS Dinámica de Dislocaciones



Representación de la caja de simulación de ParaDiS con dislocaciones en simulación del Molibdeno.



Formación de multiuniones de dislocaciones en bcc Mo.

Need good reactive empirical (fast) potentials → “chemistry”

REBO I (Reactive-Empirical-Bond-Order, $R_{\text{cut}}=2 \text{ \AA}$)

Brenner *et al.* 1990-1992. Bond-order term has 3-body contributions. No dispersion forces (long range), no repulsion/attraction term for non-bonded atoms → Graphite planes not bonded (distance between planes $\sim 3.3 \text{ \AA}$).

REBO I + (dispersion/non-bonded), $R_{\text{cut}} \sim 10 \text{ \AA}$)

Various implementations. MDCASK (LLNL): *parallel implementation (A. Kubota)*

REBO II, $R_{\text{cut}}=2 \text{ \AA}$

Brenner *et al.* 2002. Re-parametrization of Brenner I, including new functional forms

AIREBO (Adaptative-Intermolecular REBO, $R_{\text{cut}}=10 \text{ \AA}$)

Stuart *et al.*, 2000-2003: REBO I + LJ-(bond-order) + torsion (4-body)

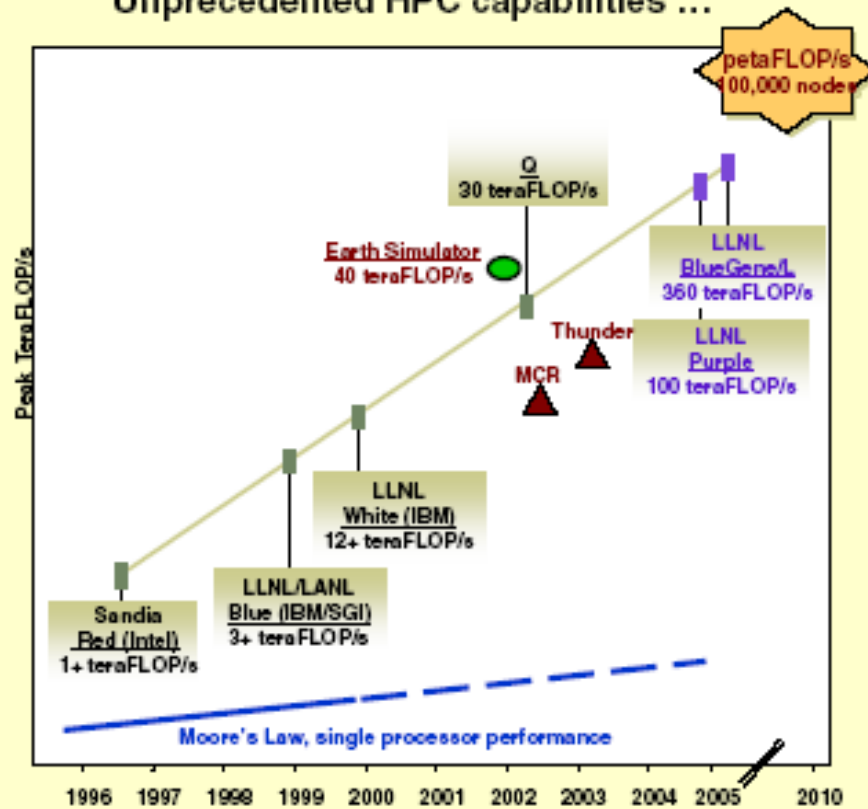
Tight-Binding based BOP ($R_{\text{cut}}=2.4 \text{ \AA}$)

Pettifor+Oleynik (1999-2003): new version has both 3 and 4 body terms. SLOW

ReaxFF [REActive Force Field, $R_{\text{cut}}=3.9 \text{ (LJ)} / \infty \text{ (Coulomb)}$]

Van Duin *et al.* (2001-2003): BOP+LJ+torsion+Coulomb. VERY SLOW, but available for several species (H,C,O,N, Si, Al,...). BRAND NEW parallel version (GRASP –SNL, P. Vashista -USC), not yet widely available.

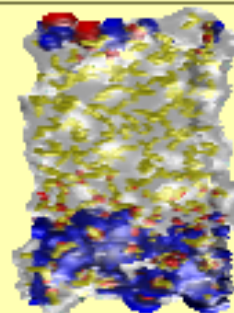
Unprecedented HPC capabilities ...



... are being used by LLNL and its collaborators to tackle exciting new scientific challenges

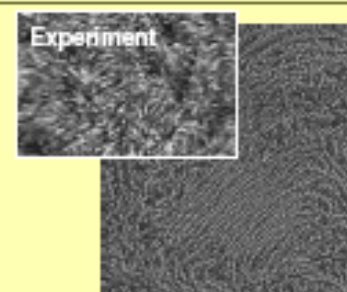
Scientific Breakthroughs

Liquid/Vapor Interface



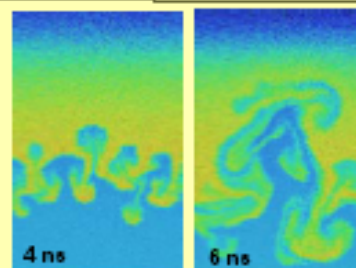
First observation of hydrogen bonding moieties
2000 CPUs, 1400000 CPU hours

Novel Polymer Materials



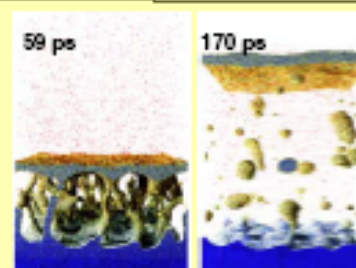
First-time observation of crystallization in polymers
2000 CPUs, 720000 CPU hours

Rayleigh-Taylor Instabilities



First fully atomistic model with dynamic ICF conditions
2000 CPUs, 96000 CPU hours

Nano-scale Fabrication



Laser-matter interactions on experimentally accessible time and space
2000 CPUs, 96000 CPU hours

Damage efficiency saturates when subcascade formation occurs

